NACA
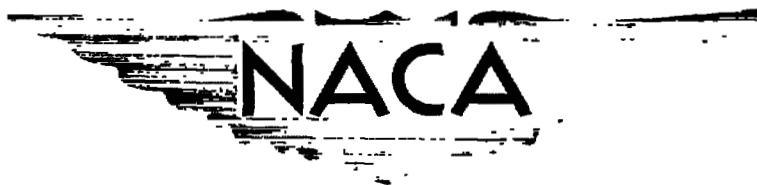
RESEARCH MEMORANDUM

SIMULATED FLIGHT INVESTIGATION OF SCALED-SPEED ELASTIC

SWEPT-WING BOMBER AND FIGHTER MODELS

COUPLED WING TIP TO WING TIP

By Robert F. Thompson

Langley Aeronautical Laboratory
Langley Field, Va.

Declassified July 17, 1962

NATIONAL ADVISORY COMMITTEE
FOR AERONAUTICS
WASHINGTON

February 14, 1956

NACA RM L55J24

NATIONAL ADVISORY COMMITTEE FOR AERONAUTICS

RESEARCH MEMORANDUM

SIMULATED FLIGHT INVESTIGATION OF SCALED-SPEED ELASTIC

SWEPT-WING BOMBER AND FIGHTER MODELS

COUPLED WING TIP TO WING TIP

By Robert F. Thompson

SUMMARY

A wind-tunnel investigation was made wherein dynamic models that included elastic simulation were used to study the flight characteristics of a swept-wing bomber with parasite swept-wing fighters coupled at the wing tips. This coupled configuration represents an efficient towing arrangement whereby the operational range of fighters can be increased. All bomber rigid-body freedoms other than roll were eliminated in the flight simulation. The models were coupled wing tip to wing tip with fighter roll freedom about the tip-coupling axis. Some fighter lateral trim was provided at all test conditions by mechanically linking the fighter ailerons to the wing tip of the bomber so as to deflect automatically in proportion to the relative bank angle between the fighter and the bomber. The effects of providing additional (to ailerons) fighter lateral-trim moments by skewing the tip-coupling axis were also studied.

Results indicated that satisfactory flight could be made to full-scale simulated speeds of about 400 miles per hour with fighter lateral trim provided only by fighter ailerons. Bomber roll freedom and the aileron deflection ratios tested had only a secondary effect on the flight characteristics. Skewing the tip-coupling axis $10°$ was slightly beneficial; however, a further increase in skew angle to $20°$ had a pronounced adverse effect. Maximum test speeds for skew angles of $0°$ and $10°$ were limited by a tendency of the fighter to twist the bomber wing and diverge in torsion. With a skew angle of $20°$, the fighter oscillated at approximately constant amplitudes about the tip-coupling axis at speeds well below the divergence speeds. The coupled-flight characteristics were little affected by coupling the fighter wing tip to the bomber wing tip by a short boom which shifted the fighter longitudinal position rearward. The limiting speeds for the coupled configuration were considerably lower than the bomber-alone flutter speeds.

INTRODUCTION

The operating range of an aircraft can be extended by towing the aircraft over some portion of the flight. In particular, fighter protection could be maintained on bombing missions beyond the normal operating range of fighters by towing the fighters as parasites to be released when protection is needed. From the standpoint of aerodynamic efficiency, the towing can perhaps best be accomplished by coupling the airplanes wing tip to wing tip. This method of coupling has been proposed because the fighters are supported by their own lifting surfaces and the effective aspect ratio of the coupled configuration is increased with a corresponding decrease in induced-drag coefficient. As a further refinement, loads produced by the fighter on the bomber can be decreased by coupling the fighter to the bomber with angular freedom provided proper fighter trim stability relative to the bomber is maintained. The feasibility of this towing arrangement has been demonstrated in the Langley free-flight tunnel (refs. 1 to 3) and in actual flight (ref. 4).

This type of coupling results in a relatively complex unconventional structure and complicates any theoretical prediction of the flight behavior. Equations of motion neglecting the elastic characteristics of the wing-tip-coupled configuration have been presented in reference 5 and, in addition, wind-tunnel tests to date have used relatively rigid models. The elastic modes of the coupled configuration would be expected to have a first-order effect on the flutter and stability characteristics as well as the wing-structure strength requirements. Therefore the present tests were made to provide information on airplanes coupled wing tip to wing tip wherein the wing elastic properties as well as the complete mass distribution were accurately scaled. Emphasis was placed on determining the maximum speed to which a particular configuration could be satisfactorily flown and the type of stability problems encountered. The tests were simplified by using a semispan bomber model and eliminating most of the bomber rigid-body freedoms. It was considered that results from this semispan test configuration could be used to corroborate future theoretical analyses; however, any complete configuration analysis would have to rationalize the effects of the eliminated rigid-body freedoms.

The investigation was made in the Langley 300 MPH 7- by 10-foot tunnel. Geometric, stiffness, and mass parameters representative of present-day operational swept-wing aircraft were incorporated into a 1/14-size scaled-speed model to give full-scale simulation at a pressure altitude of 20,000 feet. This scaling permitted testing over a wide full-scale simulated speed range. Mach and Reynolds number effects were not simulated. The test configuration provided fighter roll freedom at the coupling axis to decrease bomber bending loads and the effects of providing fighter lateral trim by ailerons and tip-coupling axis skew were investigated. The effects of bomber roll freedom were also determined.

COEFFICIENTS AND SYMBOLS

C_L lift coefficient, $\dfrac{\text{Model lift}}{qS}$ (twice model lift used for bomber model)

C_m pitching-moment coefficient referred to $0.215\bar{c}$, $\dfrac{\text{Pitching moment}}{qS\bar{c}}$

I_{xx}, I_{yy}, I_{zz} moments of inertia about body axis, lb-in.^{2}

q free-stream dynamic pressure, $\dfrac{\rho V^2}{2}$, lb/sq ft

S wing area, sq ft (twice area of semispan model)

c local wing chord, parellel to plane of symmetry, ft

$\bar{c}$ mean aerodynamic chord of wing using theoretical tip, $\dfrac{2}{S} \displaystyle\int_0^{b/2} c^2 dy$

b wing span, perpendicular to plane of symmetry, ft

y lateral distance from plane of symmetry, ft

ρ mass density of air, slugs/cu ft

V free-stream velocity, ft/sec

α angle of attack of wing-root chord, deg

α_t angle of attack of wing-tip chord, deg

θ angle of twist of wing-tip chord relative to wing-root chord, positive downward, $\alpha - \alpha_t$, deg

δ aileron deflection, measured in a plane perpendicular to aileron hinge line, deg

i_t angle of horizontal tail relative to longitudinal body axis, positive when leading edge is up, deg

ϕ relative bank angle between wing tips connecting bomber and fighter, measured in a plane perpendicular to the longitudinal body axis and considered zero at trimmed flight, deg (see fig. 1(a))

β skew angle of tip-coupling axis, angle between tip-coupling axis and longitudinal body axis, deg (see fig. 1(a))

l general dimension of length (see text on selection of scale factor)

λ scale factor for length, $\dfrac{l_M}{l_F}$

ω angular frequency, $2\pi f$, radians/sec

f frequency of oscillation, cps

w weight of wing per unit length along elastic axis, lb/in.

M_S static moment of wing about elastic axis per unit length along the elastic axis, positive indicates trailing edge down, in-lb/in.

I_α pitching moment of inertia of wing about elastic axis per unit length along the elastic axis, lb-in.^{2}/in.

EI wing bending rigidity, lb-in.^{2}

GJ wing torsional rigidity, lb-in.^{2}

Subscripts:

M refers to model

F refers to full-scale airplane

MODEL AND APPARATUS

General Description of Models

The models were chosen for this investigation so as to be representative of present-day, operational, swept-wing aircraft and the bomber was selected to have a high degree of wing flexibility. Model simulation was based on a survey of full-scale data available at the time the investigation was originated. Geometric details such as fuselage cross section and wing height were selected for model simplicity; however, plan-form geometry was considered to be closely representative. The wings were the only components in which elastic properties were accurately simulated. A sketch of the general

arrangement of the test configuration is presented in figure 1. Photographs of the model mounted in the tunnel and associated test equipment are shown in figure 2. Tests were made with a semispan bomber model and a complete fighter model. The fighter was flown in two longitudinal positions as shown in figure 1. When coupled wing tip to wing tip (fig. 1(a)), the elastic axes intersected at the wing tip; when coupled by a boom (fig. 1(b)), the fighter was shifted rearward approximately one bomber tip-chord length. Coupling the fighter by a boom would be expected to decrease the aerodynamic efficiency and was tested to determine the effects on stability.

For all tests, the fighter was coupled to the bomber with roll freedom about the coupling axis and all other fighter motions relative to the bomber were restrained by the coupling. Fighter lateral trim was provided by mechanically linking the fighter ailerons to the bomber wing tip (fig. 2(c)) so that the ailerons deflected automatically in proportion to the relative bank angle between the fighter and the bomber. The ailerons were rigged to maintain a relative bank angle of zero and deflected in the conventional manner, that is, the right aileron was up when the left aileron was down. Some additional lateral trim moment about the tip-coupling axis could have been obtained by rigging the ailerons to deflect symmetrically; however, this was not done in the present investigation. Fighter lateral trim moments supplementary to the aforesaid aileron moments were provided by skewing the tip-coupling axis as shown on figure 1(a) so that for any skew angle other than 0°, rotation of the fighter about the coupling axis resulted in a stabilizing angle-of-attack increment.

Bomber root conditions simulating symmetric and antisymmetric lateral modes were tested and are indicated schematically in figure 1(c). Symmetric mode tests were made with the bomber root locked so that the wing was cantilevered from the tunnel sidewall and there were no bomber rigid-body freedoms. An equivalent bomber-level-flight lift distribution was maintained over the bomber wing throughout the test speed range, a full-scale bomber weight of 75,000 pounds (bomber semispan model lift of 23.6 lb) being assumed. For the antisymmetric modes, the bomber was free to roll about the longitudinal body axis. In the free-to-roll tests, the lift of the bomber wing at lateral trim would necessarily be less than normal. Therefore to have the model and full-scale lift coefficients the same, antisymmetric-mode tests were also made with a statically deflected spring supplying a preload moment about the bomber roll axis, in the direction shown. The magnitude of this moment forced the bomber wing to carry an equivalent symmetric-mode lift distribution (lift = 23.6 lb) at lateral trim. The preload springs used were arranged so that the bomber-rigid-body roll frequency was extremely low. Changes in bomber bank angle obtained in these tests had little effect on the preload moment.

Selection of Scale Factors

A scaled-speed model was considered to be the most practical for the flight conditions to be simulated in this investigation. A limitation imposed on the tests was that the Mach and Reynolds number effects were not simulated. Neglecting Mach and Reynolds number, scaling of the model was based on the parameters considered significant to flutter. The model was chosen to be 1/14 the size of representative full-scale airplanes and the parameters scaled are listed in terms of the geometric scale factor λ. If l is considered to be a general dimension of length

$$\lambda = \frac{l_M}{l_F} = \frac{1}{14}$$

where the subscripts M and F refer to model and full scale, respectively. The density factor ρ_M/ρ_F was chosen to be 1.737 to provide the air-density relationship between average model test conditions and the full-scale airplanes operating at a pressure altitude of 20,000 feet. True altitude simulation based on actual test air densities did not vary more than ±500 feet from average test conditions. The parameters were scaled as follows:

Parameter	Symbol notation and scale factor
Length	$\dfrac{l_M}{l_F} = \lambda = \dfrac{1}{14}$
Velocity	$\dfrac{V_M}{V_F} = \lambda^{1/2} = 0.267$
Frequency	$\dfrac{\omega_M}{\omega_F} = \dfrac{1}{\lambda^{1/2}} = 3.75$
Weight per unit length	$\dfrac{w_M}{w_F} = \dfrac{\rho_M}{\rho_F}\lambda^2 = \dfrac{1.737}{14^2}$
Weight	$\dfrac{w_M l_M}{w_F l_F} = \dfrac{\rho_M}{\rho_F}\lambda^3 = \dfrac{1.737}{14^3}$

Parameter	Symbol notation and scale factor
Mass moment of inertia per unit length	$\dfrac{I_{\alpha_M}}{I_{\alpha_F}} = \dfrac{\rho_M}{\rho_F}\lambda^4 = \dfrac{1.737}{14^4}$
Mass moment of inertia	$\dfrac{I_{\alpha_M}l_M}{I_{\alpha_F}l_F} = \dfrac{\rho_M}{\rho_F}\lambda^5 = \dfrac{1.737}{14^5}$
Bending rigidity	$\dfrac{(EI)_M}{(EI)_F} = \dfrac{\rho_M}{\rho_F}\lambda^5 = \dfrac{1.737}{14^5}$
Torsion rigidity	$\dfrac{(GJ)_M}{(GJ)_F} = \dfrac{\rho_M}{\rho_F}\lambda^5 = \dfrac{1.737}{14^5}$

No attempt was made to design a given value of structural damping into the model. The structural damping coefficient g_h of the model bomber wing was 0.012 measured from the first bending mode and calculated according to the following relationship:

$$g_h = \frac{1}{\pi}\text{ (logarithmic decrement)}$$

This was the only damping coefficient measured; however, the type of model construction used would be expected to give relatively low values of structural damping.

Model Construction Details

General details of model construction and principal model dimensions are given in figures 3, 4, and 5.

Bomber.- The wing of the semispan bomber model was of spar-segment construction consisting of a duraluminum spar to which 19 balsa segments were attached to form the wing surfaces (fig. 3). This simple method of construction enabled close simulation of predetermined structural properties and construction details are shown in figure 5. The spar was designed to have the desired wing bending and torsion rigidity and the segments attached so as to make no contribution to the wing stiffness.

An analysis of the full-scale bomber wing stiffness distribution
to be simulated indicated that sufficiently close simulation could be
obtained with a constant ratio of bending to torsion rigidity
$\left(\frac{EI}{GJ} = 1.23\right)$. A cruciform spar cross section was chosen having the basic
dimensions shown in figure 6. This cross-section shape gave the desired
EI/GJ ratio and was about seven times as stiff in the chordwise bending
direction as in the up and down direction. The spar was linearly tapered
in three steps along its length to give the desired spanwise stiffness
distribution and was located along the wing 38-percent chord line which
was the desired elastic axis location. The variation of bending and
torsion rigidity with distance along the elastic axis is shown in
figure 6. The values given in figure 6 were verified by experimentally
loading the wing before and after the segments were attached.

A duraluminum rib was glued in the center of each balsa segment
such that the rib could be attached to the flanges of the cruciform
spar. A narrow gap was left between adjacent segments and the gap was
filled by gluing a 1/8-inch-wide strip of sponge rubber around the air-
foil section as shown in figure 5. The sponge rubber was glued to one
end of each segment and pressed against the adjacent segment when the
wing was assembled. This type of construction enabled the balsa segments
to be attached to the spar without influencing the spar stiffness. The
wing could be easily assembled and disassembled, allowing free access
to any portion of the structure. For the speed range tested, this
method of filling the gaps was satisfactory in that the sponge rubber
was not distorted by air loads. Ballast weights were added to each
balsa segment to adjust the total wing mass, mass unbalance, and mass
moment of inertia to the desired scaled values. Bomber wing weight dis-
tribution and engine nacelle data are given in figure 7. The model
engine nacelles were made of hardwood and the elastic properties of the
full-scale nacelles and supports were not simulated.

The semispan bomber fuselage had a cylindrical center section and
a faired nose and afterbody section (fig. 3). Bomber roll freedom was
provided by mounting a segment of the center fuselage section and the
wing on a ball-bearing-supported roll yoke which allowed roll freedom
about the longitudinal body axis when the cantilever lock was removed.
The mounting bracket which supported the roll yoke was bolted to the
conventional tunnel balance frame and the angle of attack of the bomber
was varied in the conventional manner. Lift of the semispan model was
measured by the tunnel balance system. Mass and inertia properties of
the bomber fuselage about the longitudinal body axis are given in table I.

Fighter.- Principal dimensions of the fighter model are given in
figure 4. Fighter construction consisted of a central steel fuselage
spar to which the wings, tail surfaces, and fuselage shell were attached.

Longitudinal trim of the fighter was provided by an all-movable hori-
zontal tail which was adjusted manually at the model. The flexible wings
were constructed in the same manner as the bomber wing. Stiffness and
mass distribution are given in figures 8 and 9. The fighter ailerons
were rigged to deflect asymmetrically in proportion to the relative bank
angle ϕ between the fighter and bomber and the ratio of aileron angle
δ to relative bank angle ϕ could be varied from about 0.6 to 1.40.
The ailerons were actuated by a mechanical linkage to the bomber wing
tip (fig. 2(d)) and a series of push-pull rods and bell cranks contained
within the fighter wing. The aileron hinges were connected to the spar
flanges similar to the manner in which the balsa segments were attached
and the ailerons were mass balanced about the hinge line. The fuselage
contour was provided by a balsa shell fastened to the fuselage spar at
two stations by through bolts and hardwood mounting ribs glued to the
balsa shell. Complete fighter weight and weight distribution is given
in table II.

Tip-Coupling Hinge

The tip-coupling hinge provided fighter roll freedom about the tip-
coupling axis and restrained all other fighter motions relative to the
bomber (fig. 2(d)). The roll axis was supported by ball bearings and the
relative angle of attack of the fighter and bomber wing tips could be
adjusted. In addition, the tip-coupling axis could be set at skew angles
of 0°, 10°, and 20° relative to the model longitudinal body axis
(fig. 1(a)). When connected by the boom, the roll axis was at the
fighter wing tip (fig. 1(b)). The gap between the model tip chords was
unsealed. The scaled mass of the tip-coupling hinge was considered to
be representative of practical full-scale applications.

Tunnel Safety Devices

In testing dynamically similar models of the type used in this
investigation, care must be taken to prevent destruction of the models
during the course of testing. Two types of safety devices were used in
conjunction with the present investigation; namely, rapid reduction of
tunnel dynamic pressure and limitation of model motion. Preliminary
tests indicated that the conventional tunnel slow down and emergency
stop procedures did not reduce the test section dynamic pressure as
rapidly as desired. Therefore a self-actuating spoiler was mounted on
the tunnel side wall, downstream of the model as shown in figure 2. The
spoiler was held closed during normal testing and, upon release, pro-
jected into the airstream, and spoiled the flow along the side wall in
the diffuser section of the tunnel resulting in a rapid reduction in
test-section dynamic pressure.

Model motion was limited by adjustable stops located above and below the model as shown in figure 2. Details of the stops are shown in figure 10. Free motion of the model could be varied by adjusting the inner cylinder relative to the outer cylinder. The stops were positioned above and below the center of gravity of the fighter and the outboard bomber nacelle. A striking bar was attached to the wing spar and located on the upper wing surface of the bomber to hit the upper bomber stop and thus prevent damage to the balsa wing segments. If the amplitude of model motion exceeded a predetermined amount, the model would hit the striking plate and force the piston against a spring. Air damping was provided so that the striking plate returned to its original position at a relatively slow rate thus preventing the spring energy from being returned to the model. The two types of safety devices used proved very satisfactory and the model was not damaged during the investigation.

Instrumentation

The model was instrumented as shown in figure 1(a) so that if flutter were encountered, the mode shapes could be determined. The output of these instruments along with tunnel dynamic pressure was recorded by a multichannel recording oscillograph. (See fig. 2(a).) In addition, motion pictures were taken simultaneously from two camera stations; one located inside the tunnel, downstream of the model (fig. 2(c)) and the other at the test-section wall opposite and slightly forward of the model.

TESTS

The tests were made through a speed range in the Langley 300 MPH 7- by 10-foot tunnel. The variation of average test Mach and Reynolds number with velocity is given in figure 11.

Still-Air-Vibration Survey

A still-air-vibration survey was made of the model to determine natural vibrational modes and frequencies. These modes serve as an added check on the inertial and elastic properties of the model and could be used in a theoretical flutter analysis of the test configuration. Photographs of the survey setup are shown in figure 12 and natural modes for the various model configurations are shown in figure 13. The model was elastically supported in a test attitude and harmonically excited over a wide frequency range. The soft elastic supports gave rigid-body suspension frequencies considerably lower than any vibrational mode frequencies. The modes were excited from several positions with

an electrodynamic shaker (shown in fig. 12 at the inboard bomber nacelle)
and for the small amount of structural damping present, natural frequen-
cies were considered to correspond to the frequency of maximum amplitude
response. Resonant frequencies were determined from oscillograph records
of the peak model response and the mode shapes were determined visually
with the aid of a stroboscope. Modes for the bomber alone were determined
with the outboard striking bar and bomber portion of the tip-coupling hinge
installed. Modes for the coupled configurations were determined with the
models coupled wing tip to wing tip with the fighter ailerons rigged for
flight. The bomber-model effective wing elastic root was perpendicular
to the elastic axis at the model center line. Adding the preloaded
springs to the free-to-roll configuration had no effect on the natural
vibration modes. All modes presented in figure 13 are normal coupled
modes and the descriptions, where given, imply predominant characteristics.
Modes higher than the ones presented generally were not clearly defined.

Wind-On Static Tests

Static tests were made to determine the aerodynamic characteristics
of the bomber and fighter separately. These data were considered necessary
so that approximate trim angles and relative wing-tip angles could be
chosen for the initial coupled-flight condition. Lift and wing-tip twist
of the bomber were measured through an angle-of-attack range with the
model cantilevered from the tunnel balance as shown in figure 3. The
fighter was mounted as shown in figure 14 and provision was made for
measuring lift, pitching moment, and wing-tip twist through an angle-
of-attack range. Wing-tip angles of both the fighter and bomber were
measured optically by using a cathetometer mounted outside the test
section to sight a target attached to the wing tip. Model static data
are presented in figure 15 for the bomber and in figure 16 for the
fighter. Jet-boundary corrections, determined by the method presented in
reference 6, have been applied to the static test angles of attack.
Blockage corrections were negligible for the present tests.

Wind-On Dynamic Tests

Tests were made through the speed range for the three bomber root
conditions shown in figure 1(c) to determine the limiting speed to which
the coupled configuration could be flown and the type of stability prob-
lems encountered. Limiting test speeds were also determined for the
bomber alone. Tests were made for coupling-axis skew angles of 0°, 10°,
and 20° and the ratio of δ/ϕ was varied from about 0.60 to 1.40. The
effects of coupling the fighter to the bomber by a boom as shown in
figure 1(b) were also determined. All flights were made with the fighter
loaded as shown in table II, with the exception of one flight made with
the external fuel tanks removed (fuel tank weight is given in fig. 9).

Coupled-configuration flights were made in the following manner: The fighter horizontal tail and the relative angle of attack of the wing tips $(\alpha_t = \alpha - \theta)$ was set for trimmed flight at a given speed. These original settings were made from static tests and once the model was flown, later adjustments were made based on visual observation of the flight behavior. The model was supported in the wind-off condition by the lower safety stops. Test section velocity was then increased until the model would lift off of the stops and fly. Varying the model angle of attack provided an additional control over the take-off velocity. Flight speed was increased until, in the opinion of the operator, safe flight could not be made at higher speeds due to approaching a stability boundary. The model was trimmed as the flight speed increased and it was necessary to shut down the tunnel to adjust the relative wing-tip angle and fighter horizontal-tail setting. The first flights for a configuration were made with the safety stops set fairly close to the model but after familiarization with the flight characteristics, the stops were moved away from the model to allow plenty of flight space. For the root-locked and free-plus-spring tests, the bomber lift was kept constant at 23.6 pounds as the test speed was increased to simulate a full-scale level-flight condition. Bomber lift for the free-to-roll root configuration was just enough to support the bomber wing in a horizontal tunnel position. The operator was provided an additional control over the model lateral trim for bomber-roll freedom tests by a lever attached to the bomber root. This lever was used as a quick-acting lateral control and once a trimmed condition was established, no lever force was applied when determining the flight behavior.

Motion pictures and oscillograph records were taken at various times throughout the speed range. No model disturbing techniques were used; however, flight observations indicated sufficient model disturbance in so-called steady flight to give the test operator a good visual indication of model stability.

<h2 style="text-align:center">RESULTS AND DISCUSSION</h2>

Results of the present investigation are summarized in the chart in figure 17. Maximum test speeds obtained for the various model configurations and a description of the model flight characteristics which limited the test speeds are presented. A motion picture showing some of the model test characteristics has been prepared as a supplement to the present paper and is available on loan from NACA Headquarters, Washington, D. C.

Bomber Alone

Maximum test speed of the bomber alone was limited by flutter for all three root conditions tested. As shown in figure 17, the symmetric (or root locked) flutter speed was slightly lower than the antisymmetric (or root free) flutter speed and the latter was not affected by the addition of the root spring to the model. The speeds listed were considered to be the lowest values at which flutter was well established. The symmetric configuration fluttered in what appeared to be a combined bending and torsion mode at a frequency of 9.1 cps and the amplitude was divergent. The antisymmetric configuration fluttered at a frequency of 9.5 cps in predominantly a chordwise bending mode (wing tip moved fore and aft). This mode did not appear to build up in amplitude very rapidly. In addition, the symmetric flutter characteristics were not affected by reducing the semispan model lift from 23.6 pounds to 0.

Fighter Coupled Wing Tip to Wing Tip

Data presented in figure 17 for the fighter and bomber coupled wing tip to wing tip were obtained with δ/ϕ ratios near 1.0. The bomber root condition generally had little effect on the maximum speeds obtained. Satisfactory model flight characteristics existed for all flight speeds below those listed. The term "satisfactory flight" is used to indicate a trimmed flight condition that appeared to be fairly steady and to have a good degree of stability. With fighter lateral trim provided only by fighter ailerons ($\beta = 0^\circ$), satisfactory flight was made to full-scale simulated speeds of about 400 miles per hour. Skewing the tip-coupling axis 10° in a direction to provide additional (to ailerons) fighter lateral trim moments was slightly beneficial; however, a further increase to $\beta = 20^\circ$ had a pronounced adverse effect.

$\beta = 0^\circ$ and $\beta = 10^\circ$.- The maximum test speed for $\beta = 0^\circ$ and $\beta = 10^\circ$ was limited by a fairly rapid decrease in model stability as the speed was increased near the values given in figure 17. Based on visual observations, the deterioration in stability was believed to be caused by approaching the critical speed for torsional divergence. This divergence tendency, while nonoscillatory in nature, was somewhat erratic and was characterized by a tendency of the fighter, when disturbed, to twist the bomber wing until the fighter reached a fairly high attitude (α > trim) and then abruptly pitch down through the trim angle of attack before returning to a normal attitude (α = trim). Attempts to alleviate this condition by changes in fighter trim were unsuccessful. A sweptback wing is usually considered to be divergence free; however, it is conceivable that the present coupled configuration could diverge due to the large external (to bomber wing) driving torque that could be contributed by having the fighter aerodynamic center well ahead of the wing elastic axis. The limiting test speed for $\beta = 10^\circ$ was slightly higher than for

$\beta = 0°$ and the divergence tendency was somewhat more oscillatory in
nature. However, emphasis should not be placed on small test speed dif-
ferences shown in figure 17 since the tests were terminated on the judg-
ment of the test operator and there was no positive indication of the
actual proximity to a stability boundary. Varying δ/ϕ from 0.60 to
1.40 had no measurable effect on the torsional-divergence boundary for
either $\beta = 0°$ or $\beta = 10°$; however, for satisfactory flight conditions,
the fighter when disturbed, returned to lateral trim more rapidly at the
higher δ/ϕ ratios. The fighter loading was changed for the test con-
dition indicated in figure 17 by removing the external fuel tanks, how-
ever, there was no apparent effect on the flight characteristics.

$\underline{\beta = 20°}$.- With a tip-coupling skew angle β of $20°$, the model
became neutrally stable at speeds roughly one-half the divergence speeds
at the lower skew angles. The term "neutral stability" is used here to
indicate approximately constant amplitude oscillations of the fighter
about the tip-coupling axis. The motion appeared to be combined pitching
and rolling of the fighter coupled with some bending or rolling of the
bomber wing depending on the bomber root condition. Bomber root restraint
(the spring was considered to apply some root restraint) had a tendency
to lower the test speed at which neutral oscillations first occurred.
The model response in this mode was not particularly violent insofar as
model safety was concerned and the test speed was increased into the
neutrally stable region, as shown in figure 17, for the root-free-plus-
spring configuration. Increasing the test speed from 64 miles per hour
to 88 miles per hour did not alter the mode of oscillation but increased
the frequency from 1.5 cps to 1.8 cps. For the other bomber root con-
ditions, neutral oscillations occurred at a frequency of 1.6 cps at
64 miles per hour with the root locked and at a frequency of 1.8 cps at
85 miles per hour with the root free. This indicates that the fighter
oscillation frequency was a function of test speed and not bomber root
condition. However, bomber root condition did have an effect on fighter
response amplitude. With the root free (including free plus spring) and
for $\delta/\phi = 0.92$, the fighter oscillated over an amplitude of $\phi \approx \pm 6°$
and increasing the test speed from 64 miles per hour to 88 miles per
hour had no effect on the oscillation amplitude (frequency was increased).
With the bomber root locked at a test speed of 64 miles per hour, there
was a tendency for the fighter oscillation amplitude to increase from
$\phi \approx \pm 4°$ to $\phi \approx \pm 15°$ until the fighter motion would get out of phase
with the bomber wing-bending motion thus reducing the amplitude and the
cycle would then repeat in a periodic manner. This effect of bomber root
condition on fighter oscillation amplitude appeared to be a result of the
manner in which the fighter motion was influenced by the bomber-wing
elastic mode for the symmetric or root-locked configuration and by the
bomber-wing mass influence for the antisymmetric or root-free configura-
tions. Neither the neutral oscillation boundary speed nor frequency was
affected by changing the δ/ϕ ratio from 0.65 to 1.20; however, the
fighter response amplitude was affected. At a test speed of 64 miles per

hour for the free-plus-spring root condition, increasing δ/ϕ from 0.65 to 1.20 decreased the fighter oscillation amplitude from $\phi \approx \pm 9^\circ$ to $\phi \approx \pm 5^\circ$. The neutral oscillation frequency was lower than any model wind-off natural frequency and the motion appeared to be predominantly a fighter-stability mode modified by the bomber wing mass or elastic influence.

Fighter Coupled on Boom

In an attempt to increase the model divergence speed, the fighter was coupled to the bomber by a boom which shifted the fighter longitudinal position approximately one bomber tip-chord length rearward (fig. 1). This decreased the moment arm between the fighter aerodynamic center and the bomber-wing elastic axis. However, as shown in figure 17, a shift in fighter position of this magnitude had no appreciable effect on the stability boundaries. In addition, the steady-flight characteristics below the speeds listed in figure 17 were very similar to the steady-flight characteristics when coupled wing tip to wing tip.

CONCLUSIONS

A dynamically similar model study was made to determine the maximum speed at which flight could be simulated for a particular coupled-airplane configuration. Full-scale-wing elastic properties were accurately simulated. The swept-wing bomber and swept-wing fighter were coupled wing tip to wing tip with fighter roll freedom about the coupling axis. Results indicated the following conclusions:

1. Satisfactory flight was made to full-scale simulated speeds of about 400 miles per hour with fighter lateral trim provided only by fighter ailerons. Bomber roll freedom and variation in aileron deflection to relative bank angle ratio from 0.60 to 1.40 had only secondary effects on the flight characteristics.

2. Skewing the tip-coupling axis 10° in a direction to provide additional (to ailerons) fighter lateral trim moments was slightly beneficial; however, a further increase in skew angle to 20° had a pronounced adverse effect.

3. Maximum test speed for skew angles of 0° and 10° was limited by approaching the critical speed for torsional divergence; with a skew angle of 20°, the model became neutrally stable at speeds well below the divergence speeds.

4. The coupled-model flight characteristics were little affected by coupling the fighter wing tip to the bomber wing tip by a boom which shifted the fighter longitudinal position approximately one bomber wing-tip chord length rearward.

5. The limiting speeds for the coupled configuration were considerably lower than the bomber-alone flutter speeds.

Langley Aeronautical Laboratory,
    National Advisory Committee for Aeronautics,
        Langley Field, Va., November 9, 1955.

B

REFERENCES

1. Bennett, Charles V., and Boisseau, Peter C.: Free-Flight-Tunnel
    Investigation of the Dynamic Lateral Stability and Control Charac-
    teristics of a High-Aspect-Ratio Bomber Model With a Sweptback-
    Wing Fighter Model Attached to Each Wing Tip. NACA RM L52E08, 1952.

2. Bennett, Charles V., and Cadman, Robert B.: Free-Flight-Tunnel
    Investigation of the Dynamic Lateral Stability and Control Charac-
    teristics of a Tip-to-Tip Bomber-Fighter Coupled Airplane Config-
    uration. NACA RM L51A12, 1951.

3. Bennett, Charles V., and Cadman, Robert B.: Free-Flight-Tunnel
    Investigation of the Dynamic Lateral Stability and Control Charac-
    teristics of a High-Aspect-Ratio Bomber Model With Self-Supporting
    Free-Floating Fuel Tanks Attached to the Wing Tips. NACA RM L51E17,
    1951.

4. Anderson, Clarence E., Jr.: Pilot's Comments on Wing-Tip Coupling
    of Aircraft. Memo. Rep. No. MCRFT - 2283, Air Materiel Command,
    Flight Test Div., U. S. Air Force, Apr. 20, 1950.

5. Schy, Albert A.: Derivation of the Equations of Motion of a Symmet-
    rical Wing-Tip-Coupled Airplane Configuration With Rotational Free-
    dom at the Junctures. NACA RM L51G12, 1951.

6. Swanson, Robert S., and Toll, Thomas A.: Jet-Boundary Corrections
    for Reflection-Plane Models in Rectangular Wind Tunnels. NACA
    Rep. 770, 1943. (Supersedes NACA WR L-458.)

TABLE I

BOMBER FUSELAGE MASS DATA

Moment of inertia about longitudinal body axis, lb-in.^{2} 59.4
Static moment about longitudinal body axis (rolls
   right semispan wing to the left), in-lb 10

TABLE II

COMPLETE FIGHTER MODEL MASS DATA

$\left[\text{Includes external fuel tanks}\right]$

Weight, lb 10.3
Center-of-gravity location, mean aerodynamic chord 0.215
I_{xx} , lb-in.^{2} 340
I_{yy} , lb-in.^{2} 590
I_{zz} , lb-in.^{2} 905

Tunnel wall

Reflection plate

Instrumentation
● Bending and torsion gage
■ Accelerometer
▲ Angle indicator

Elastic axis

Skew angle, β
0° 10° 20°

Elastic axis

Tip coupling axis

ϕ-Relative bank angle
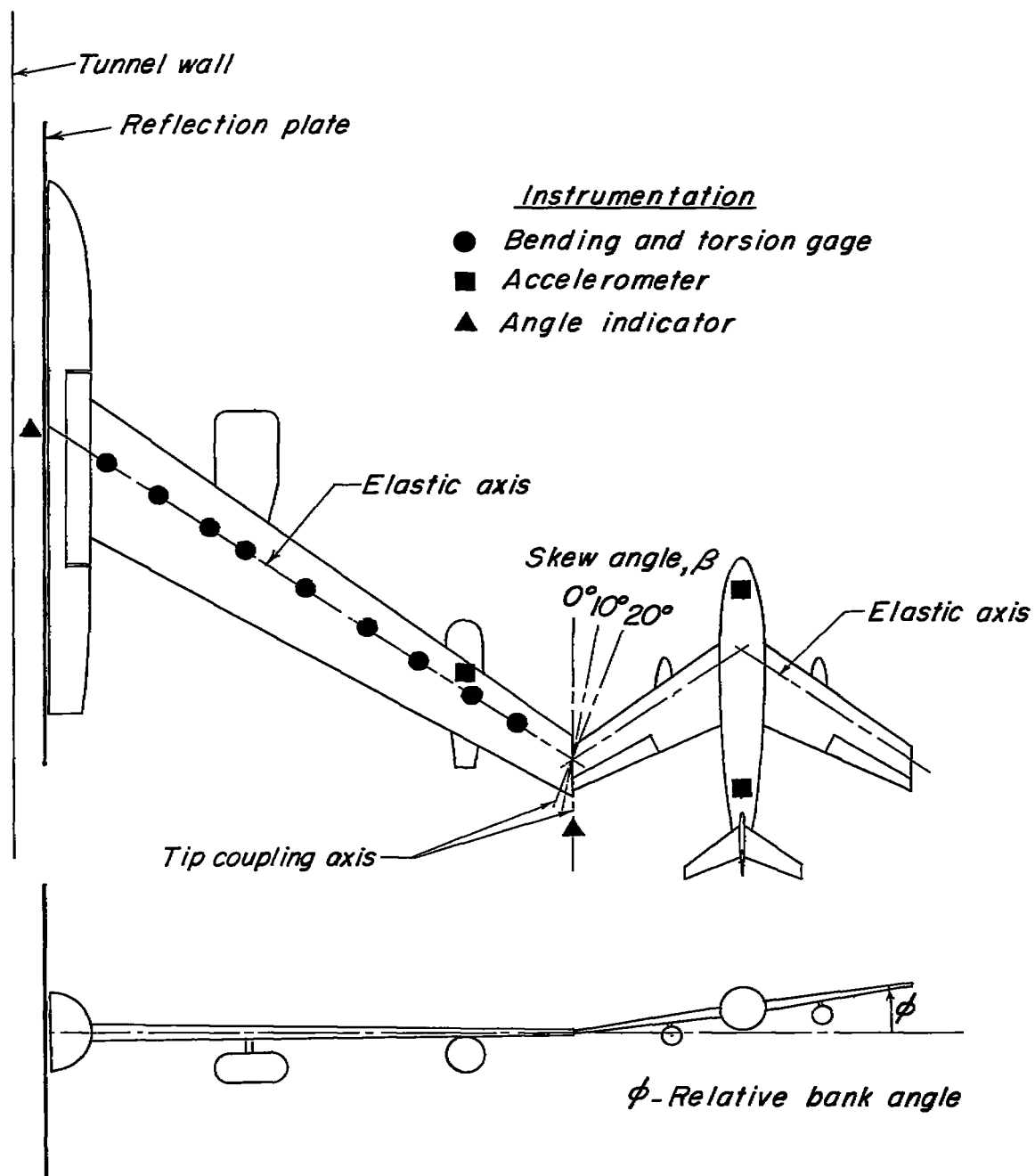
(a) Fighter coupled to bomber, wing tip to wing tip.

Figure 1.- Sketch of test configurations.
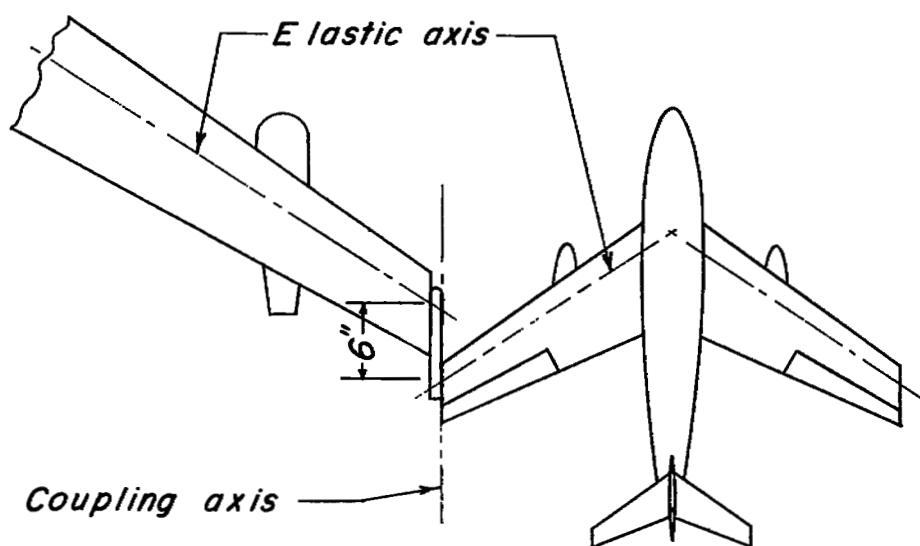
(b) Fighter coupled to bomber by boom.
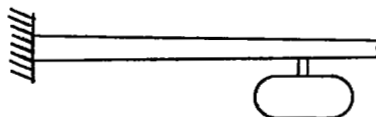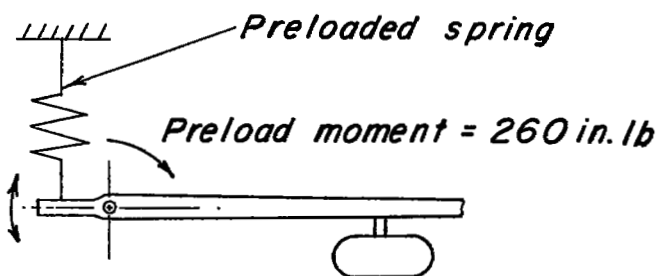
(c) Bomber root conditions tested.

Figure 1.- Concluded.
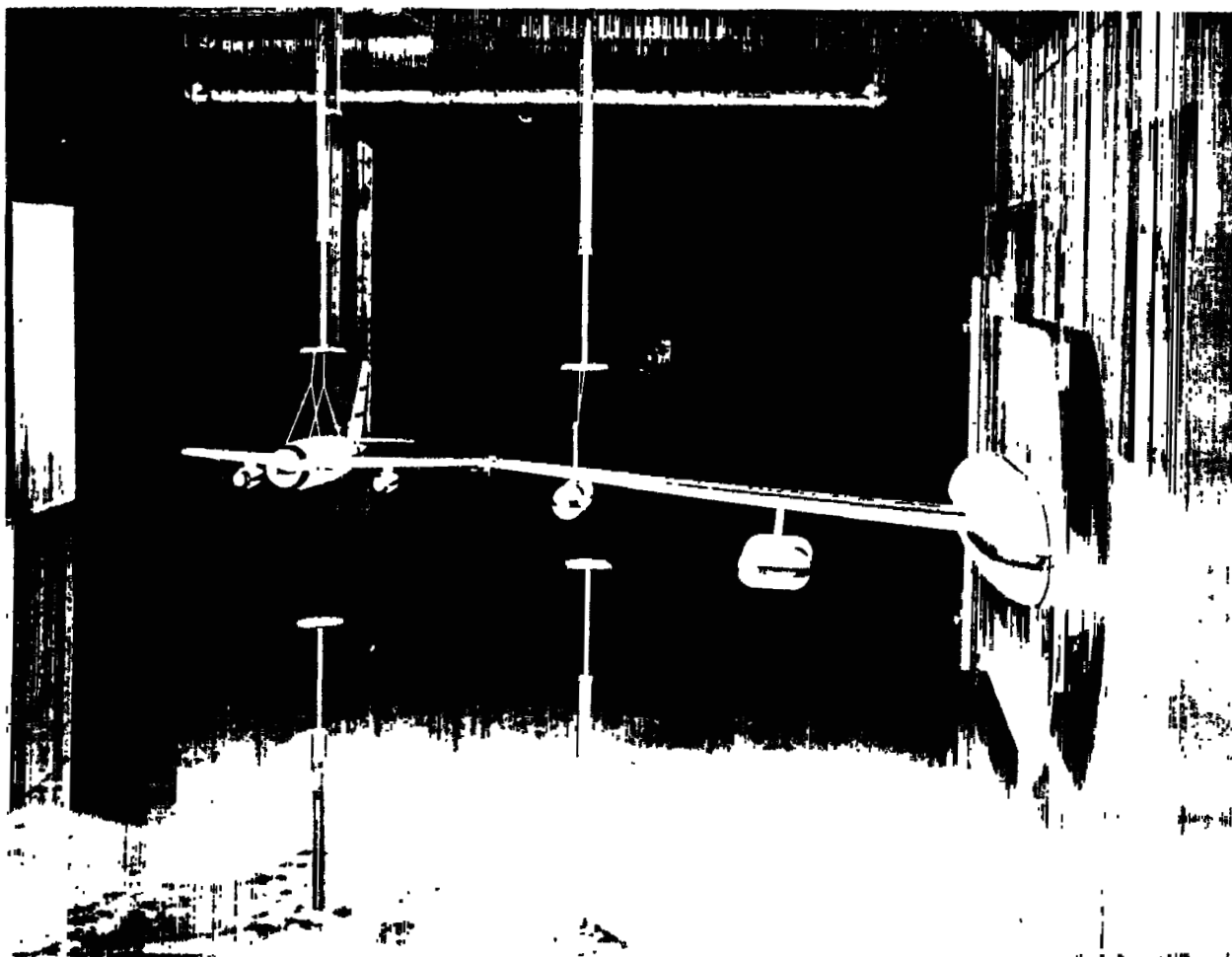
(a) Model as viewed from upstream in tunnel.

L-79952

Figure 2.- Photographs of the model.
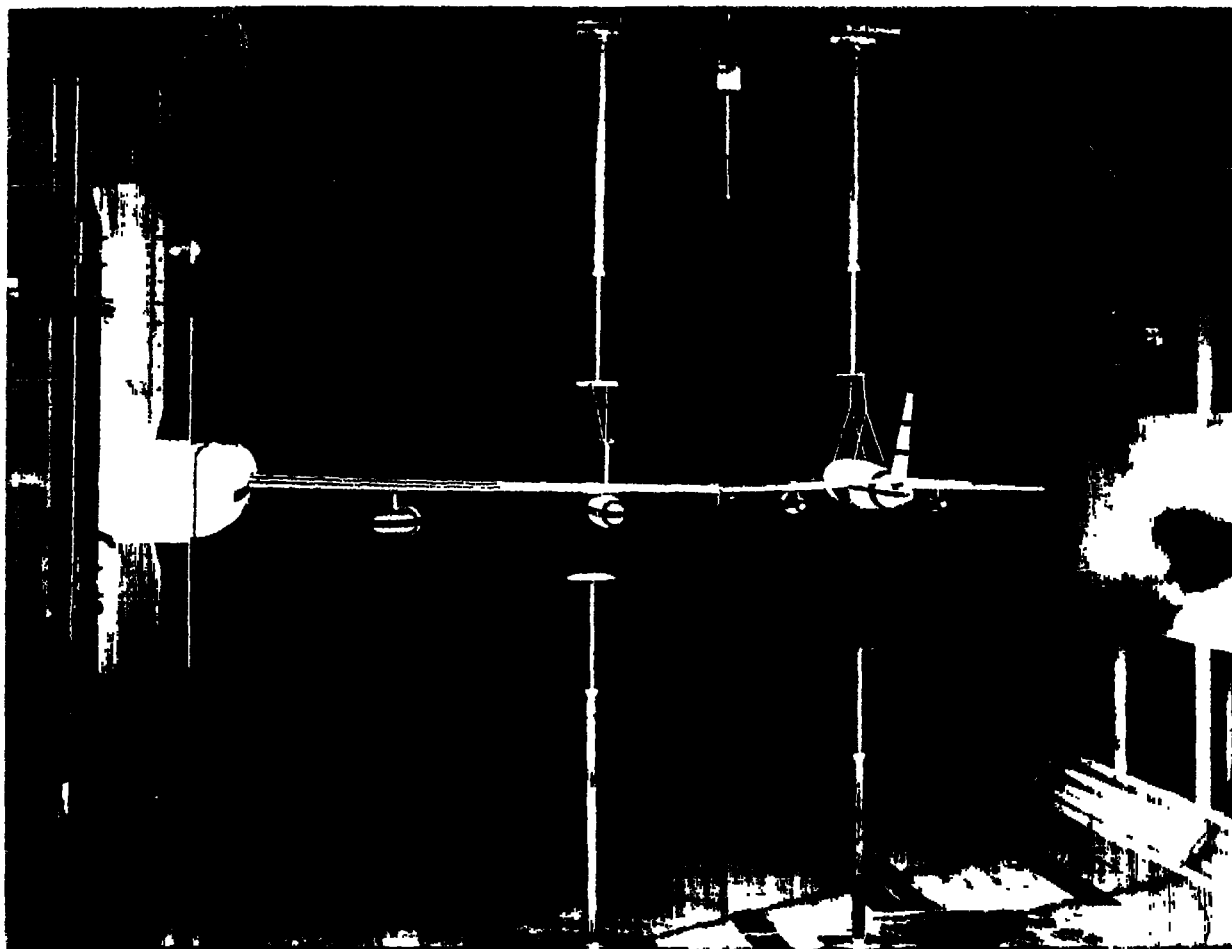
(b) Model as viewed from downstream in tunnel.　L-79951

Figure 2.- Continued.
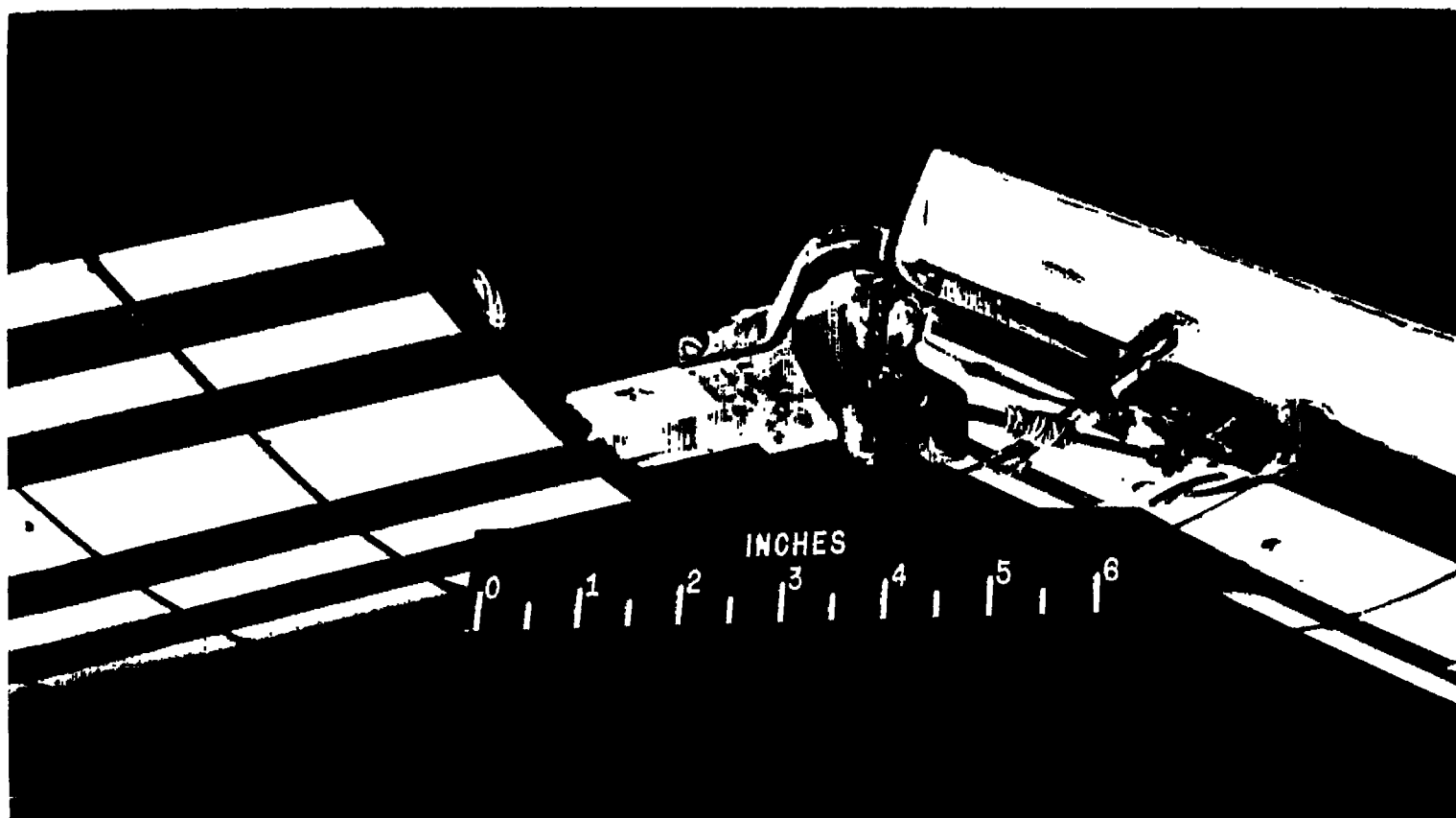
L-90434

(c) Tip-coupling details. Bomber wing-tip segment has been removed.

Figure 2.- Concluded.
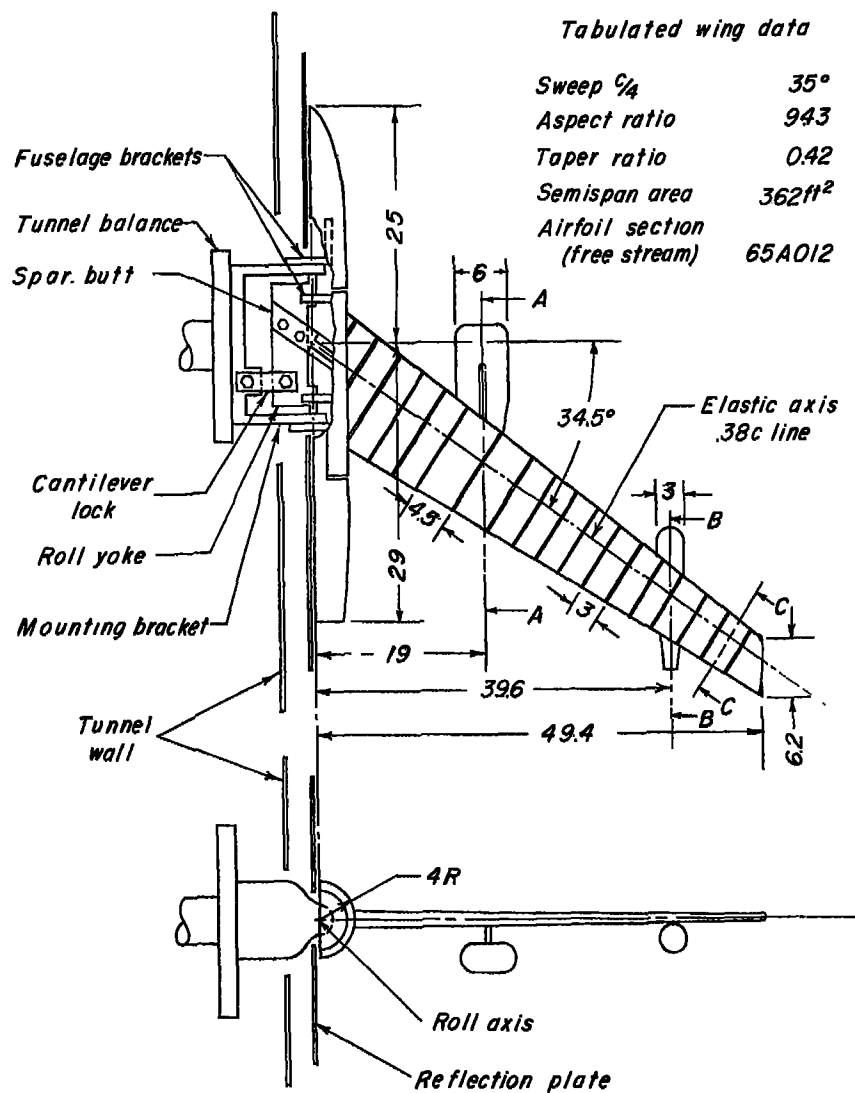
Tabulated wing data

Sweep c/4	35°
Aspect ratio	9.43
Taper ratio	0.42
Semispan area	362 ft²
Airfoil section (free stream)	65A012

Fuselage brackets

Tunnel balance

Spar. butt

Cantilever lock

Roll yoke

Mounting bracket

Tunnel wall

34.5°

Elastic axis .38c line

Nacelle attached to spar flanges at this point

Elastic axis

c.g.

Section A-A
Inboard nacelle

Nacelle attached to spar flanges at this point

Elastic axis

c.g.

Section B-B
Outboard nacelle

4R

Roll axis

Reflection plate

Attachment screw

Ballast weights

Balsa segment

Rib

Spar

Section C-C

Figure 3.- Drawing of semispan bomber model and tunnel mounting details.
All dimensions are in inches.

Tabulated data

Wing
Aspect ratio 4.8
Taper ratio 0.51
M.A.C. .... 0.575 ft
Area .... 1.48 ft²
Airfoil section
(free stream) 65A012

Empennage
Airfoil section
(free stream) 65A008

Fuselage Ordinates	
Distance from nose	Radius
0	0
0.5	0.69
1.0	1.00
2.0	1.36
4.0	1.78
8.0	2.10
12.0	2.15
16.0	2.10
20.0	1.93
24.0	1.60
28.0	1.03
31.4	0.46

Tank attached to spar flanges at this point

Aileron hinge line

Elastic axis

.25c line

c.g. located at 0.215č
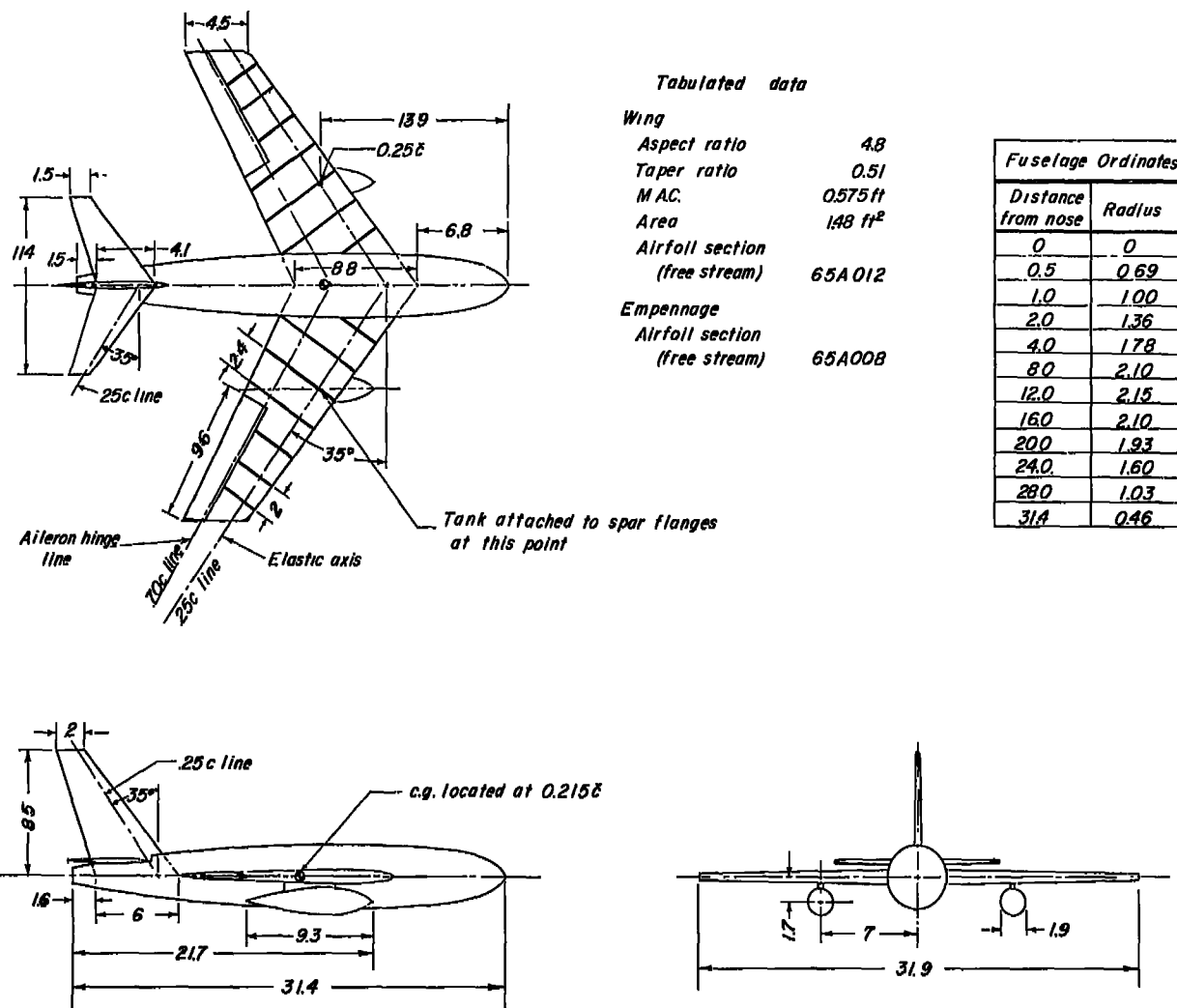
Figure 4.- Principal dimensions of the fighter model. All dimensions are in inches. Fighter weight given in table II.

Balsa segments

Rib

Glue joint

Ballast weight

Sponge rubber

Spar
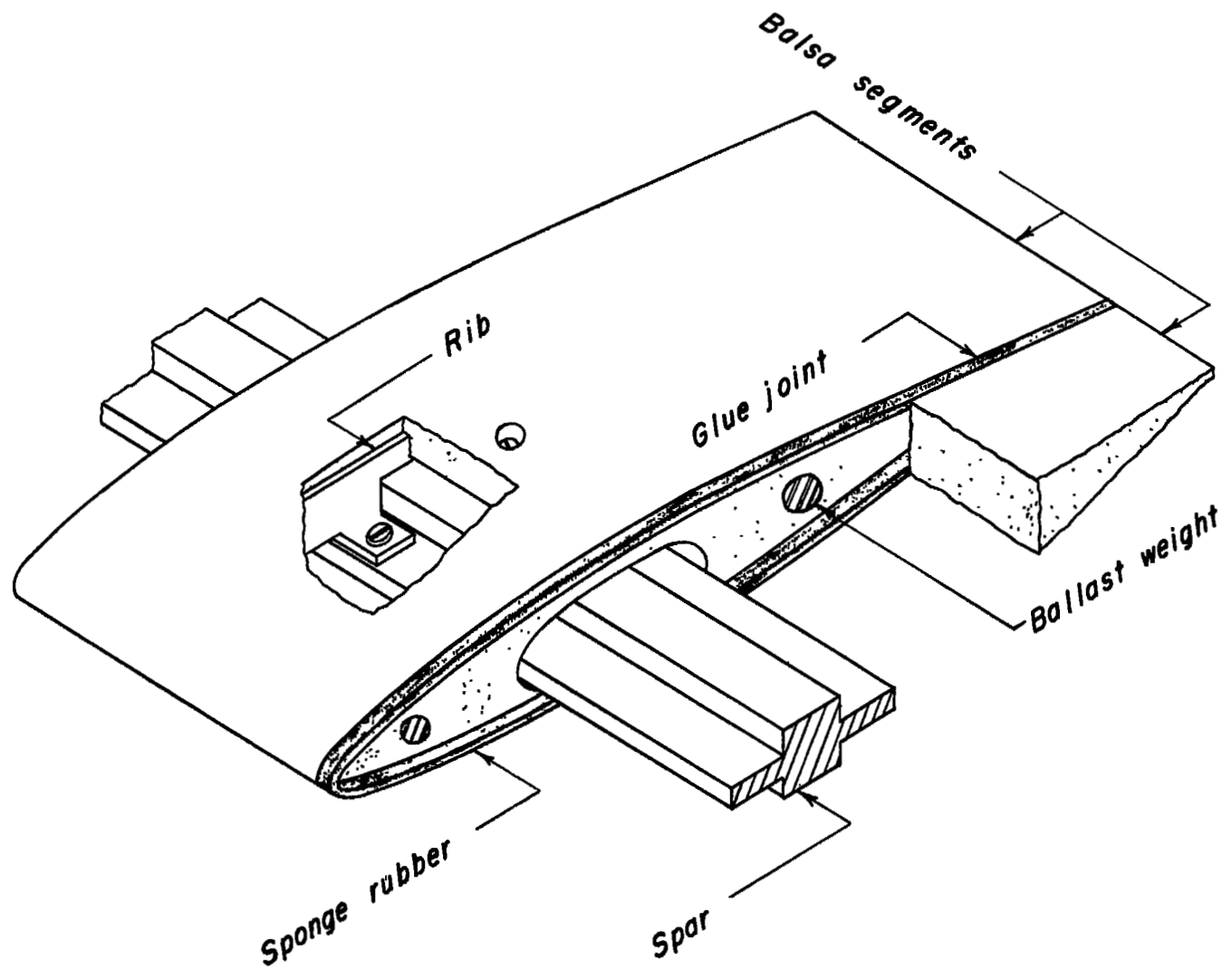
Figure 5.- Sketch showing wing construction.
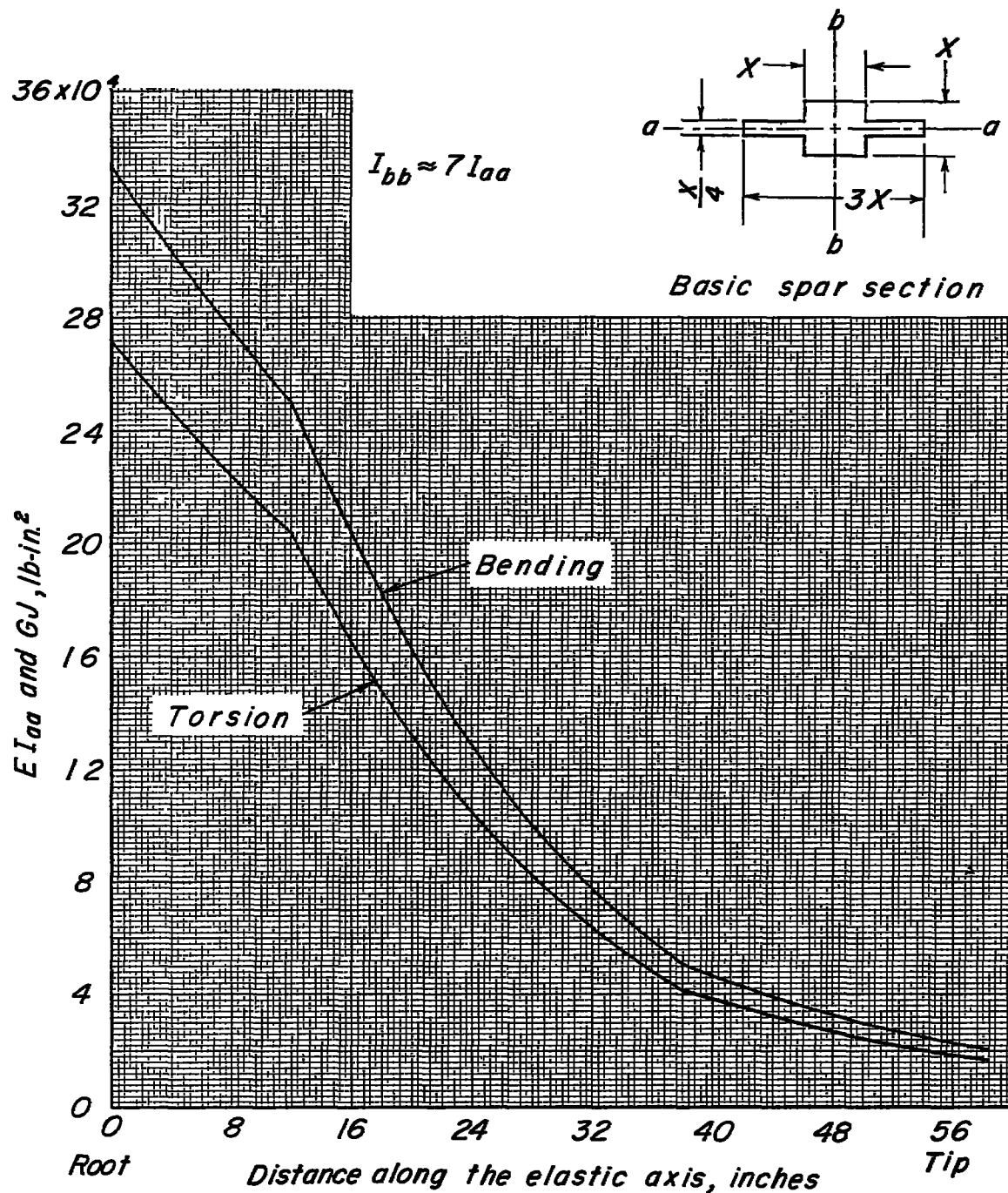
Figure 6.- Variation of bending and torsion rigidity of bomber wing with distance along elastic axis.
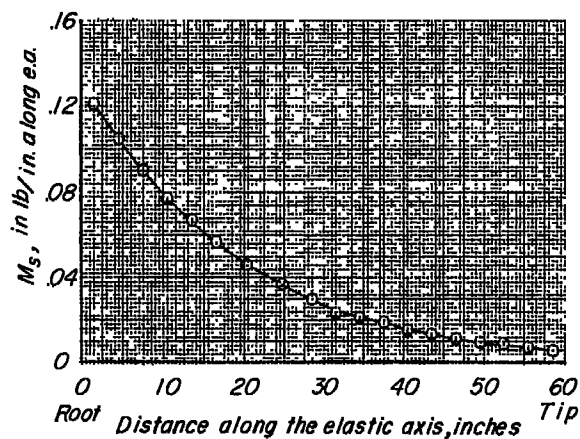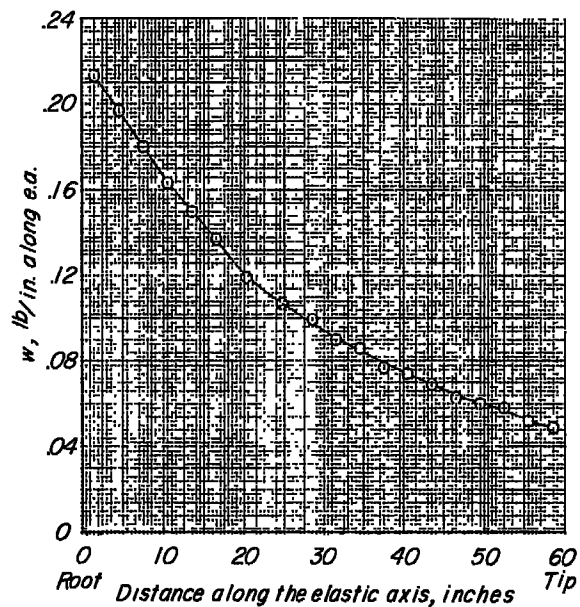
Engine Nacelle Data

	Inboard	Outboard
Distance along ea to attachment point	23 in.	48 in.
Weight	4.9 lb	21 lb
Static moment about e.a. (nose down)	-29.3 in.lb	-2.2 in.lb
Moment of inertia about e.a.	323.2 lb.in²	401 lb in²
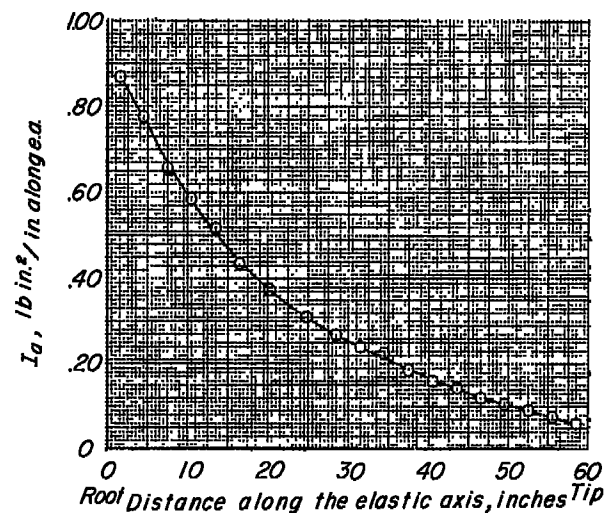
Figure 7.- Bomber wing-weight distribution.

$$I_{bb} \approx 7 I_{aa}$$
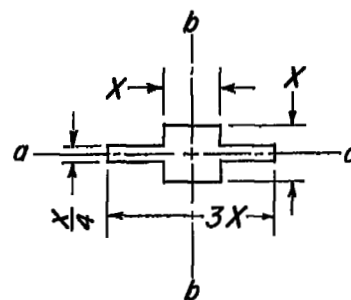
Basic spar section
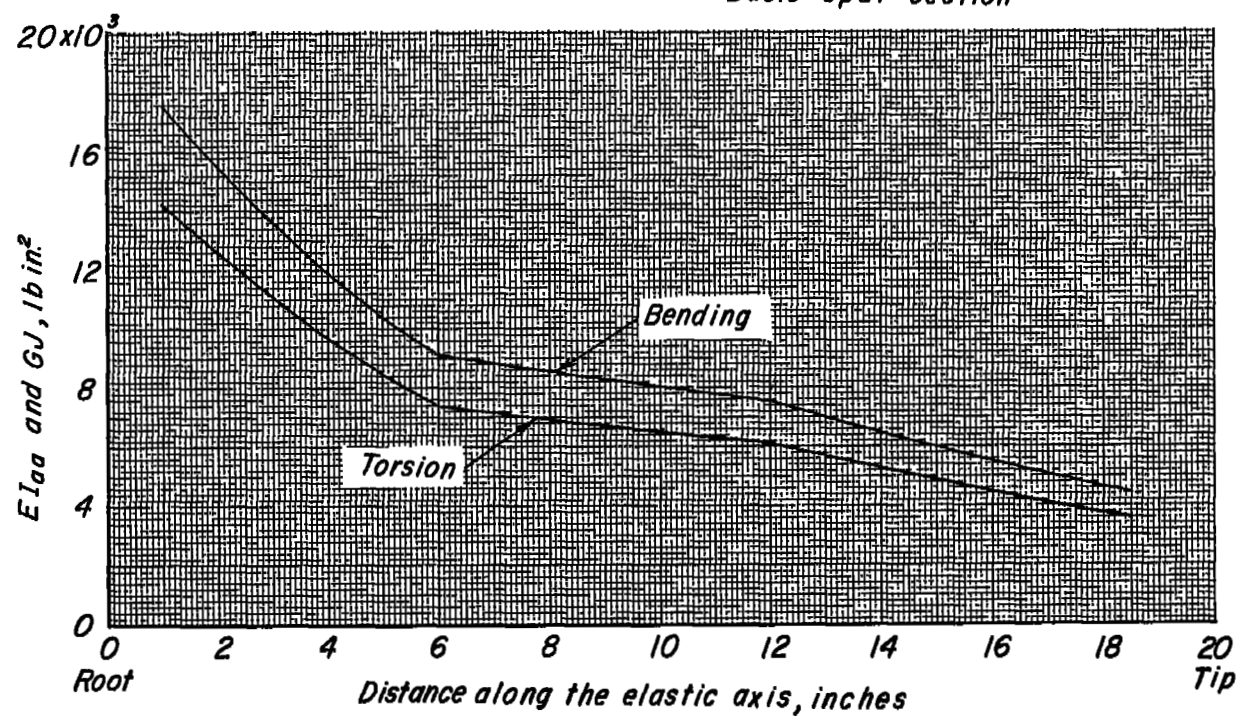
Figure 8.- Variation of bending and torsion rigidity of fighter wing with distance along elastic axis.
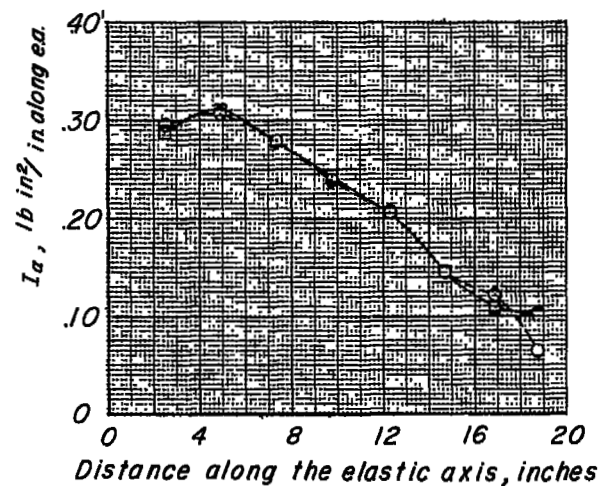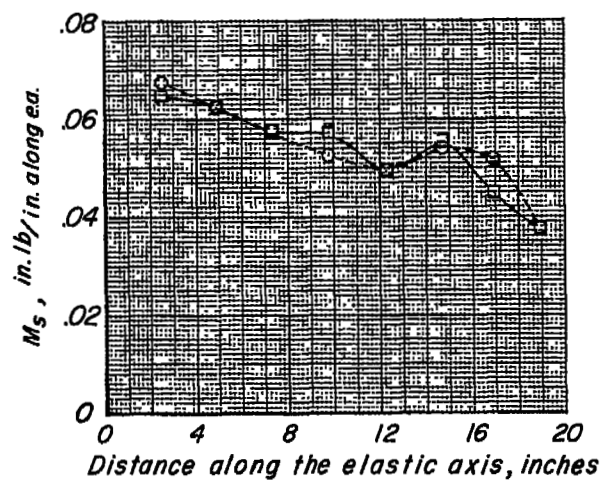
Figure 9.- Fighter wing-weight distribution.

Sponge rubber

Striking plate

Air vent

Piston

Leather bushing

Spring

Inner cylinder

Set screw

Air vents

Outer cylinder

Tunnel floor or ceiling
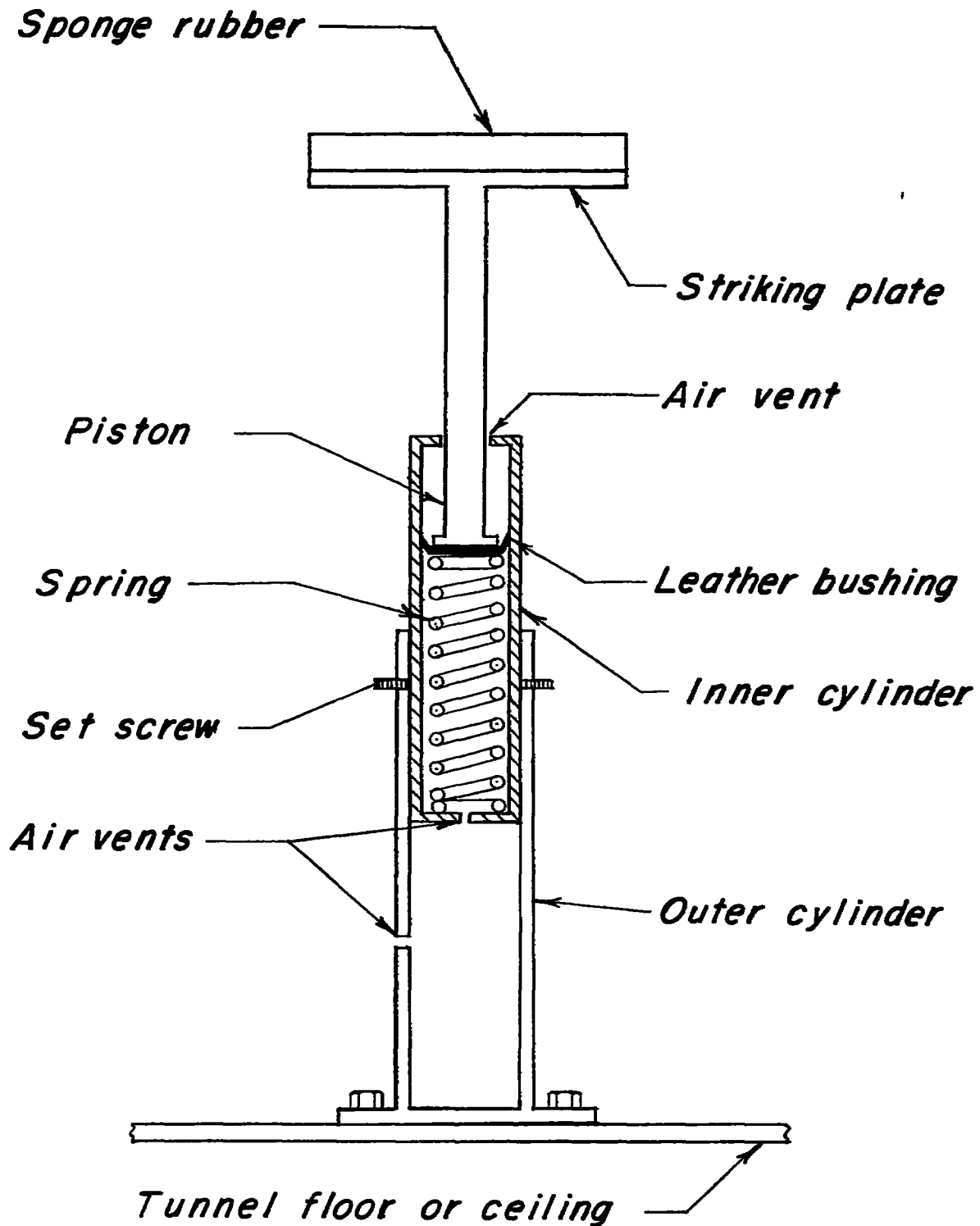
Figure 10.- Sketch of safety stops used to limit model motion.
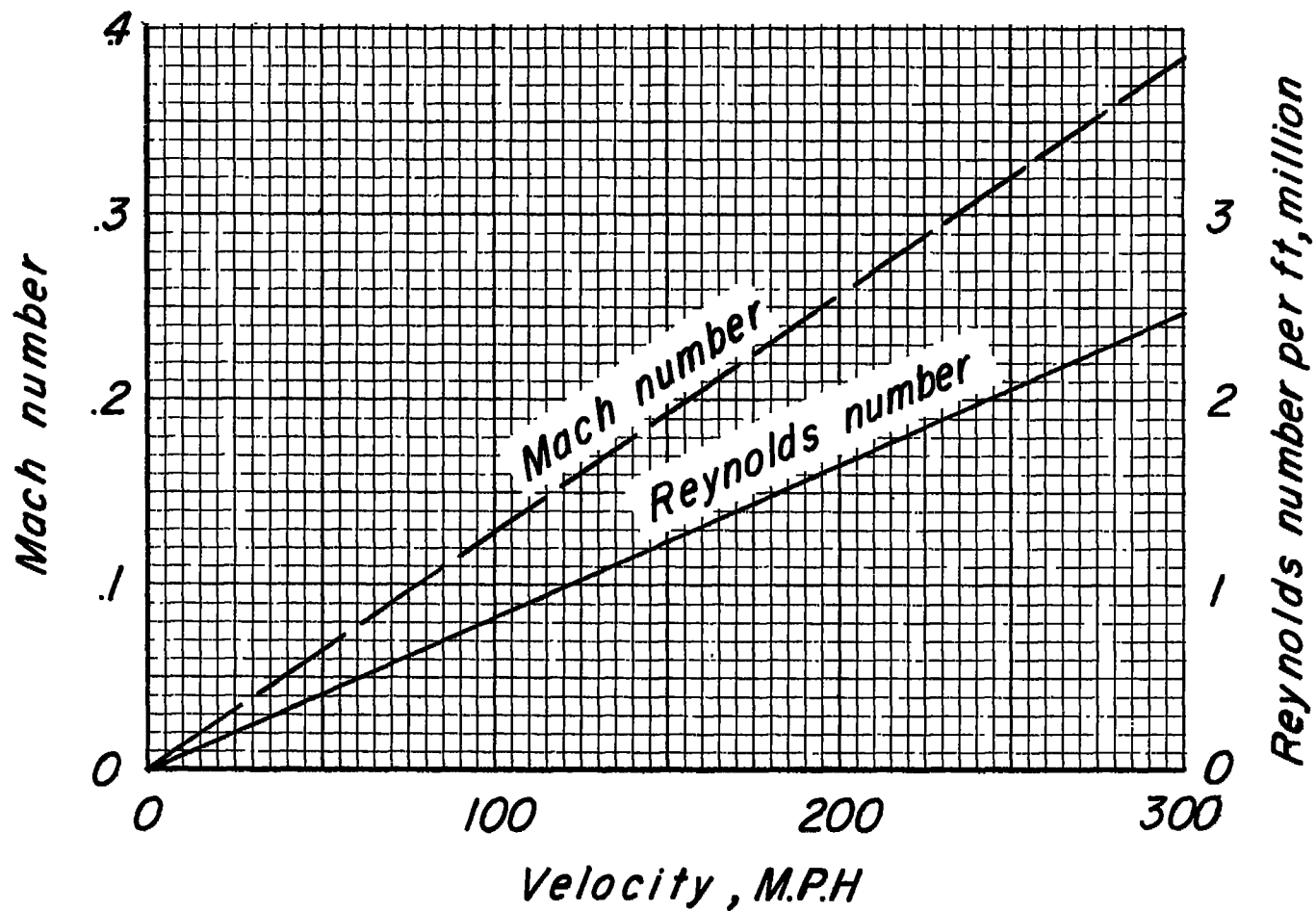
Figure 11.- Variation of average test Mach and Reynolds number with test velocity.
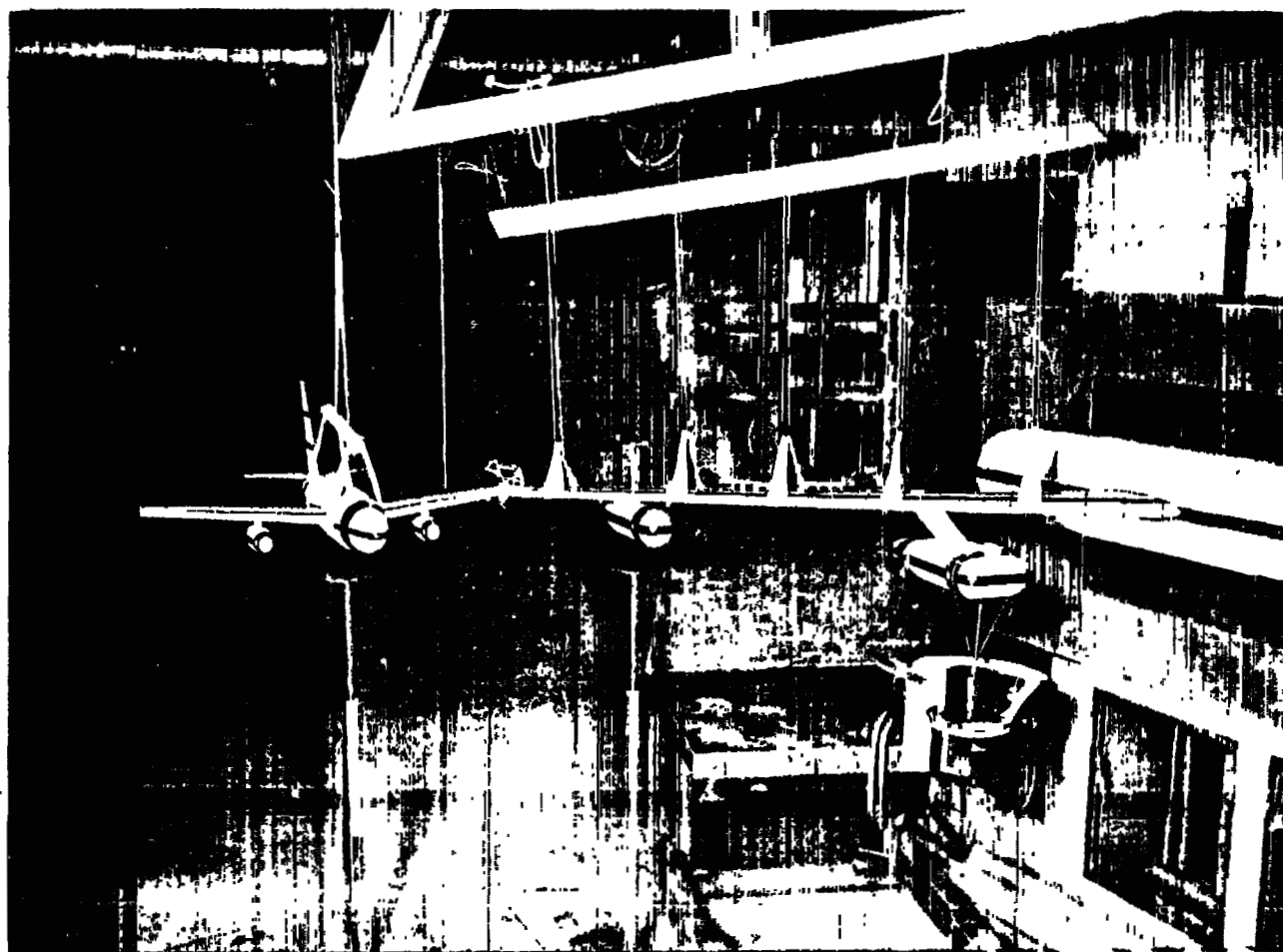
L-79963

(a) View from upstream in tunnel.

Figure 12.- Model rigged for still-air vibration survey.
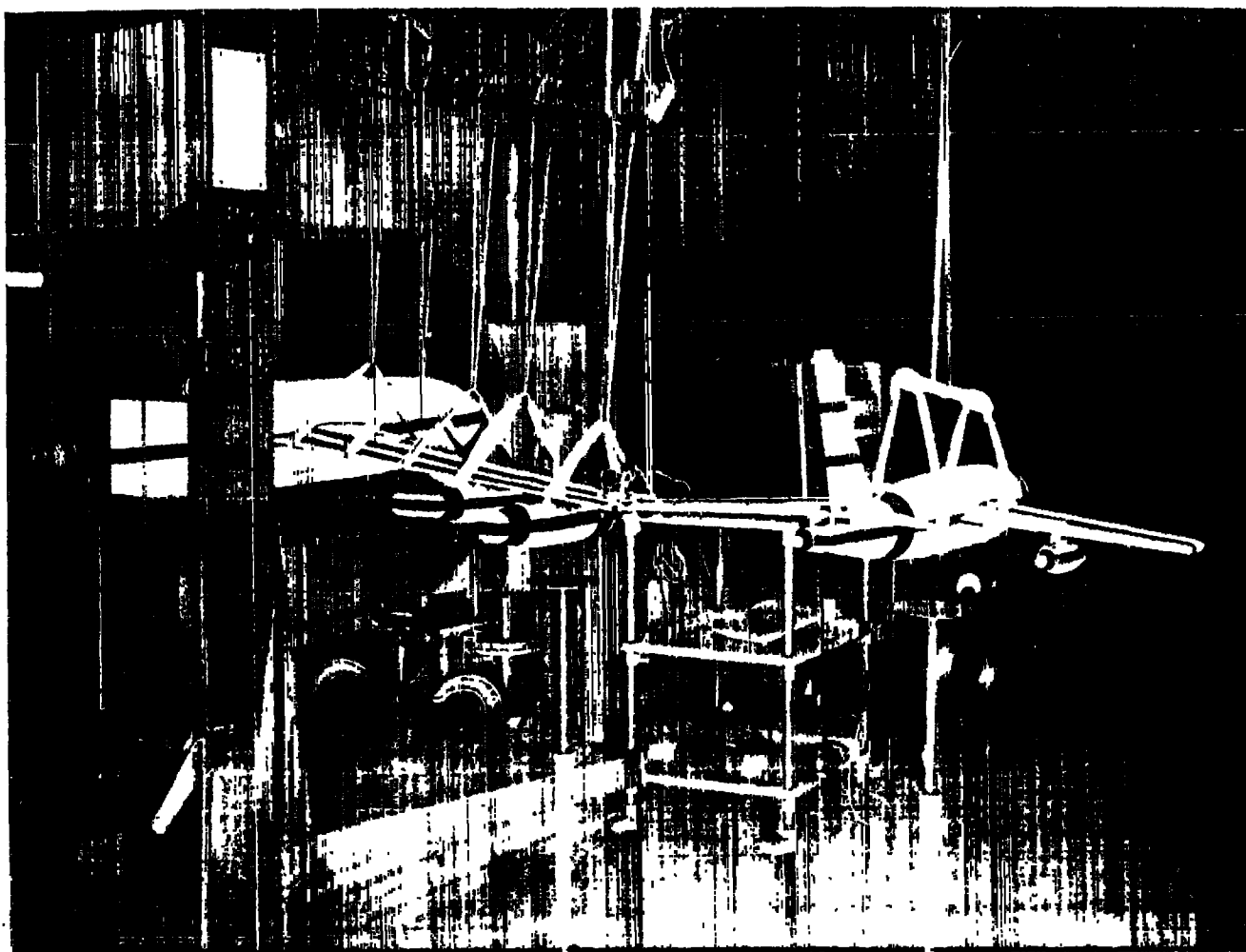
(b) View from downstream in tunnel.

L-79962

Figure 12.- Concluded.
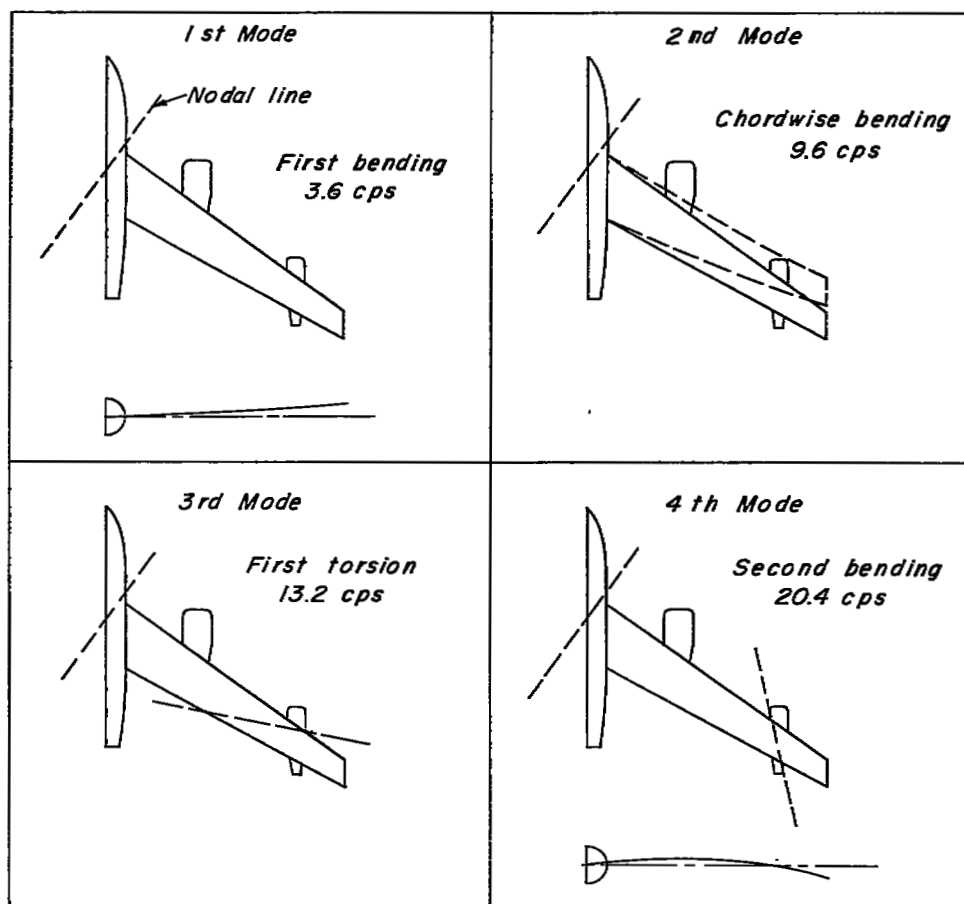
(a) Bomber alone, root locked.

Figure 13.- Still-air natural vibration modes of test model.
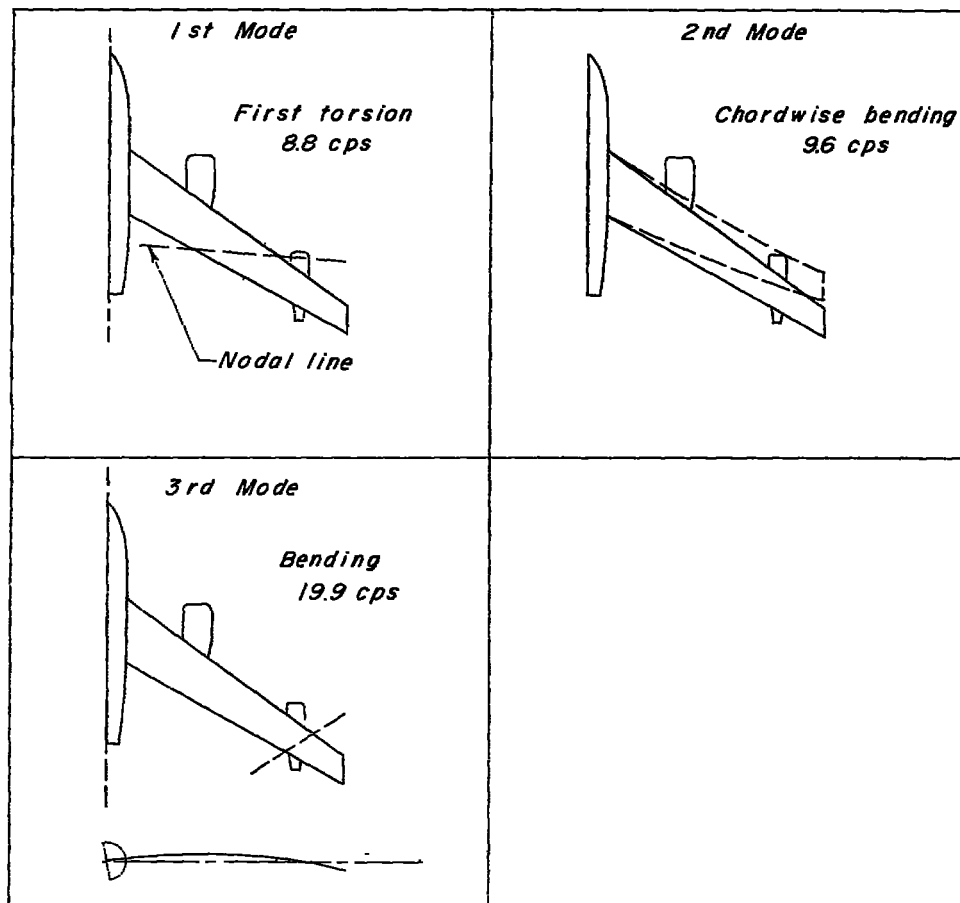
(b) Bomber alone, free to roll and free to spring.
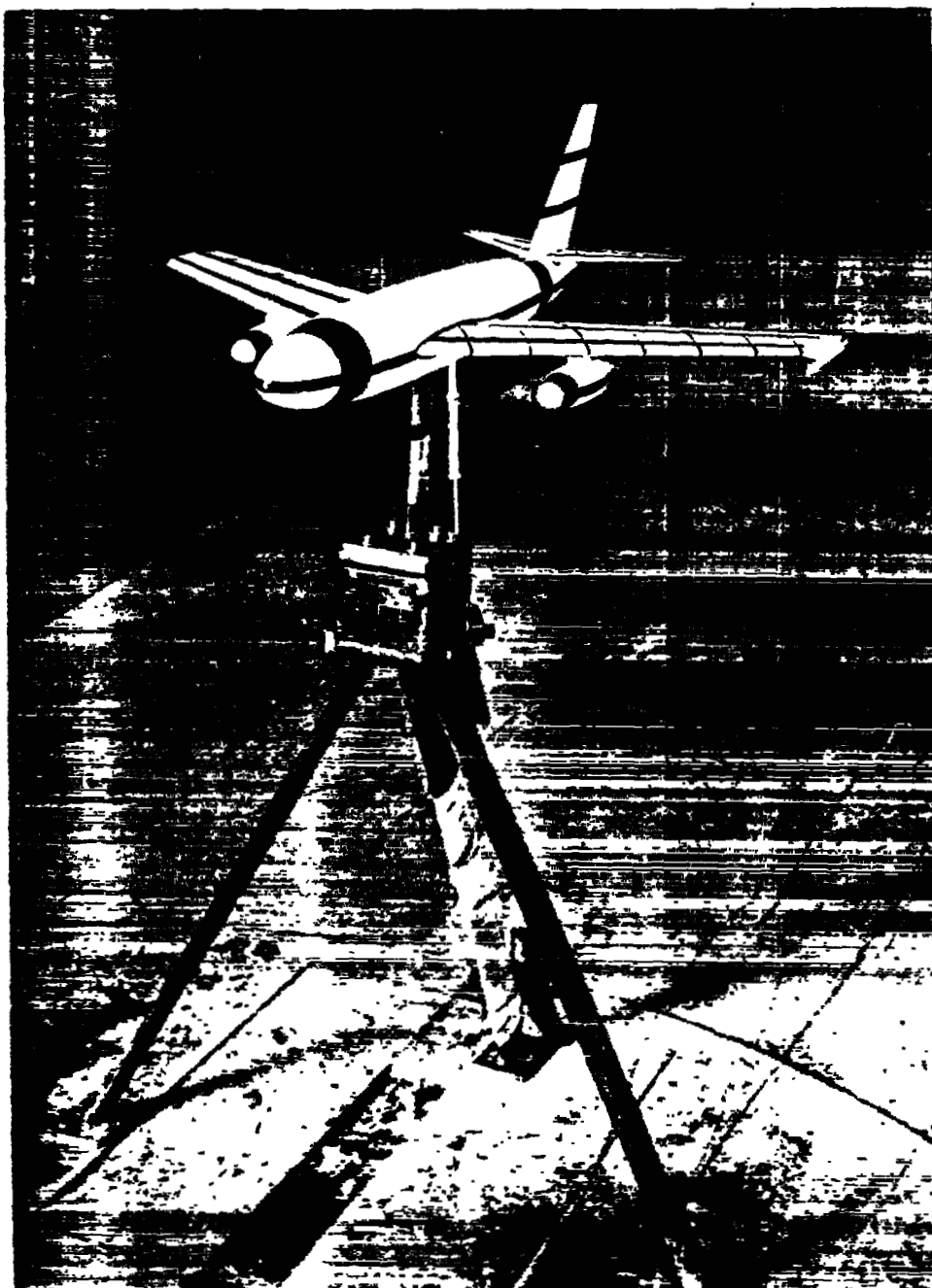
Figure 13.- Continued.
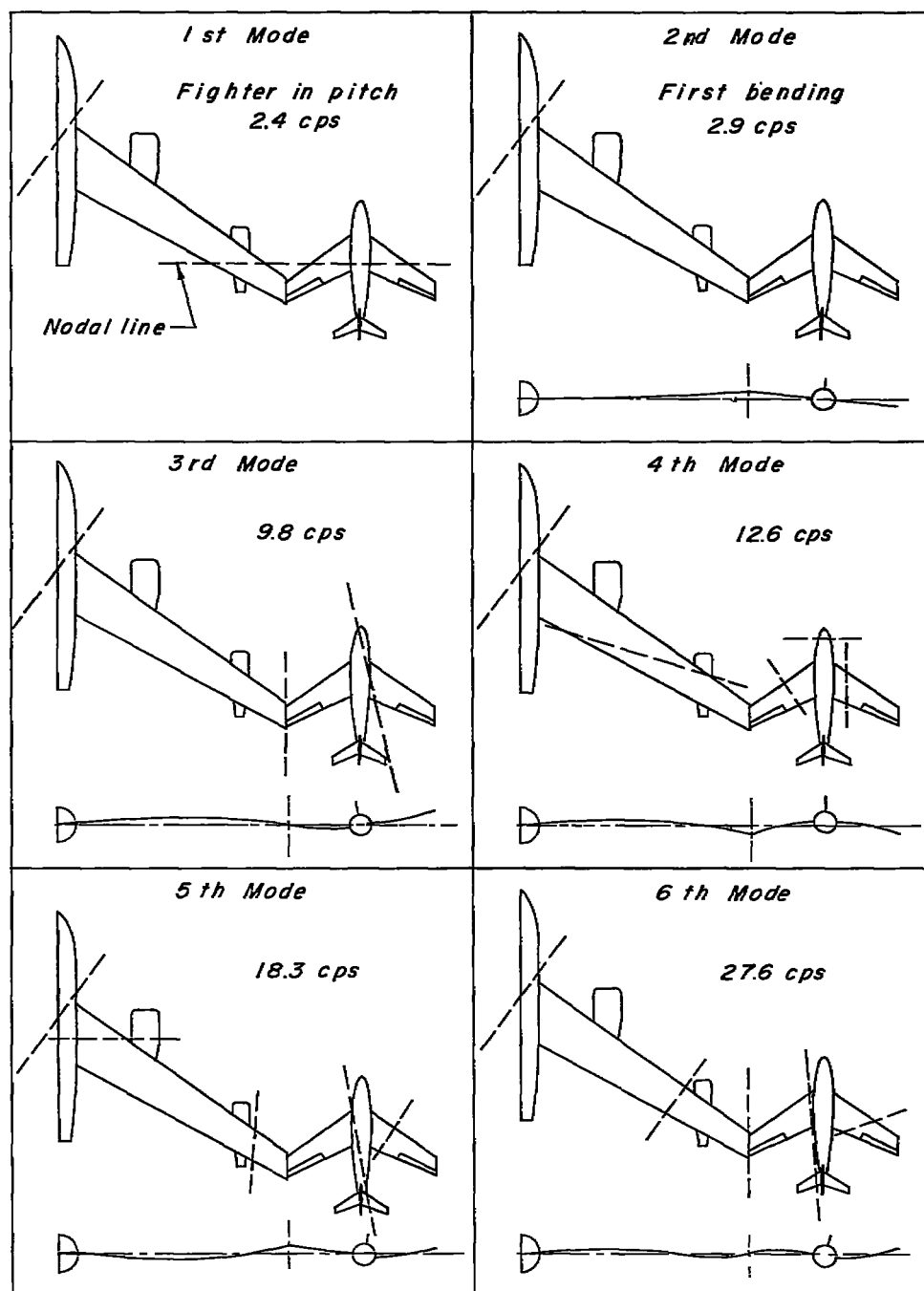
(c) Models coupled, wing tip to wing tip. Bomber root locked.

Figure 13.- Continued.
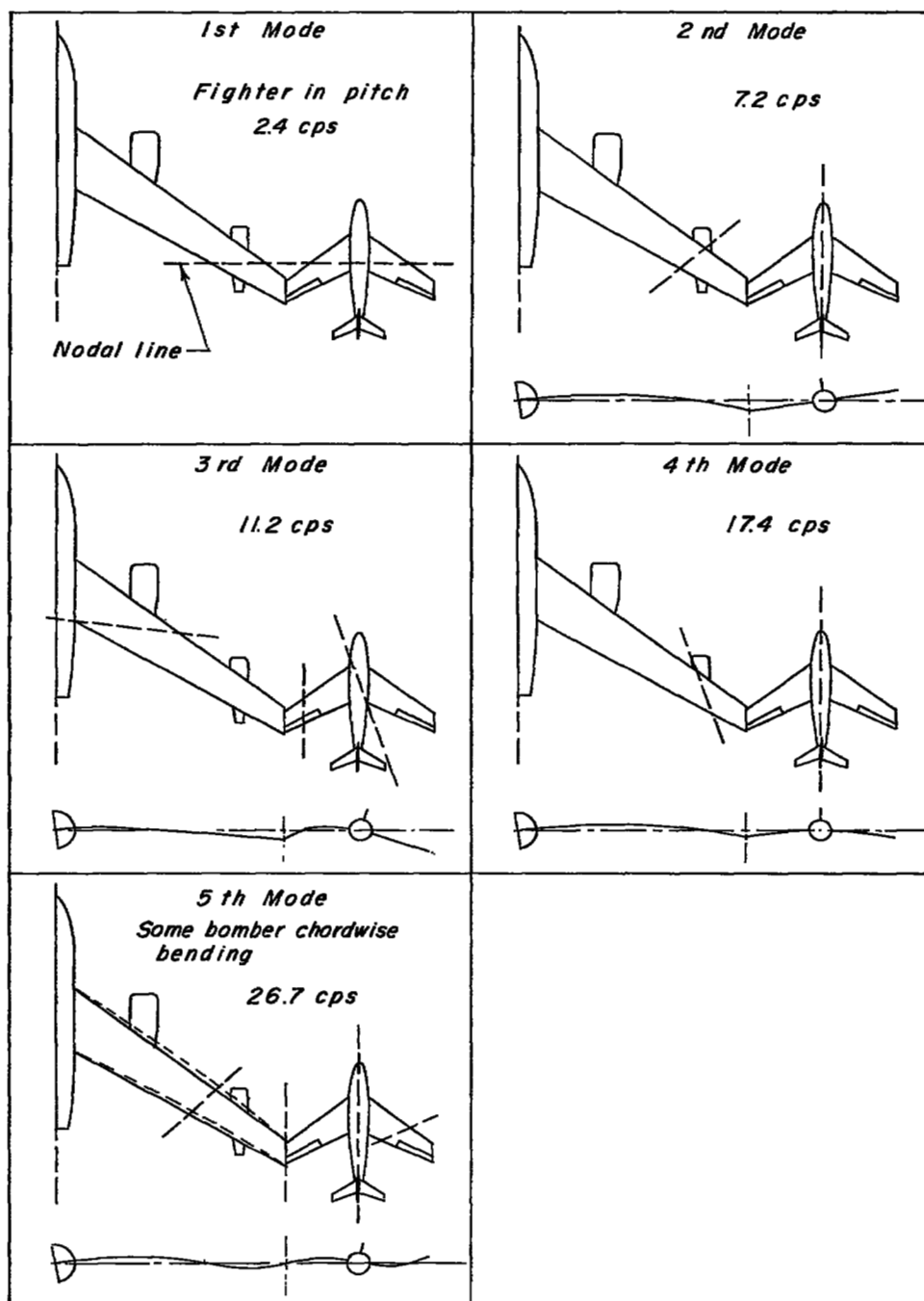
(d) Models coupled, wing tip to wing tip. Bomber free to roll and root free to spring.

Figure 13.- Concluded.

(a) View from upstream in tunnel.

Figure 14.- Fighter model mounting for static tests.

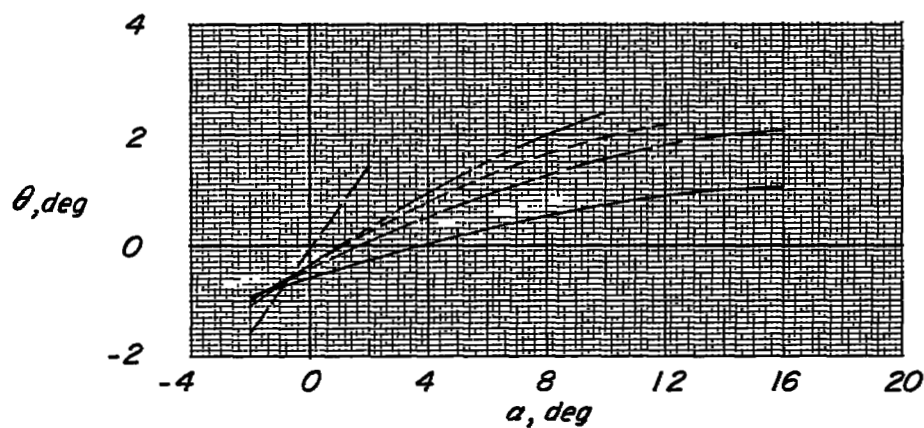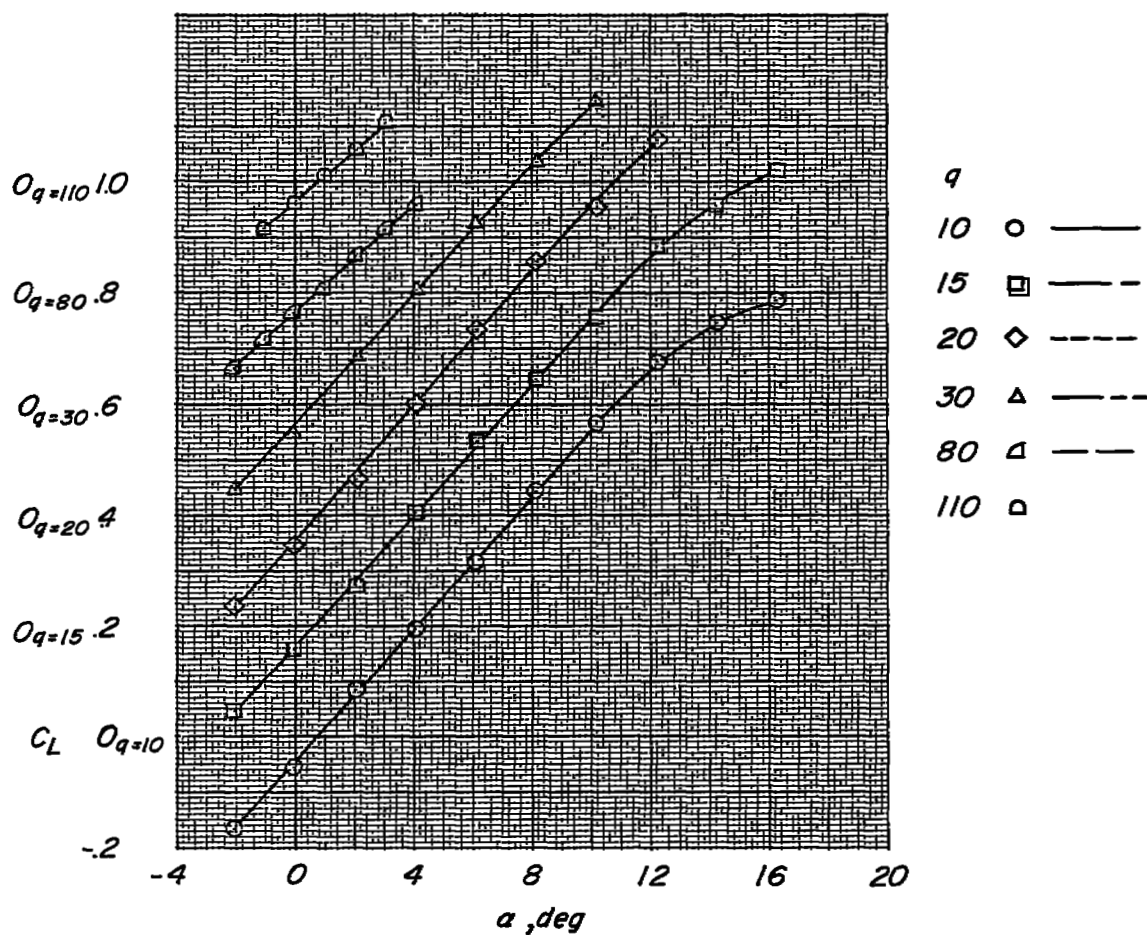(b) View from downstream in tunnel.   L-79714

Figure 14.- Concluded.

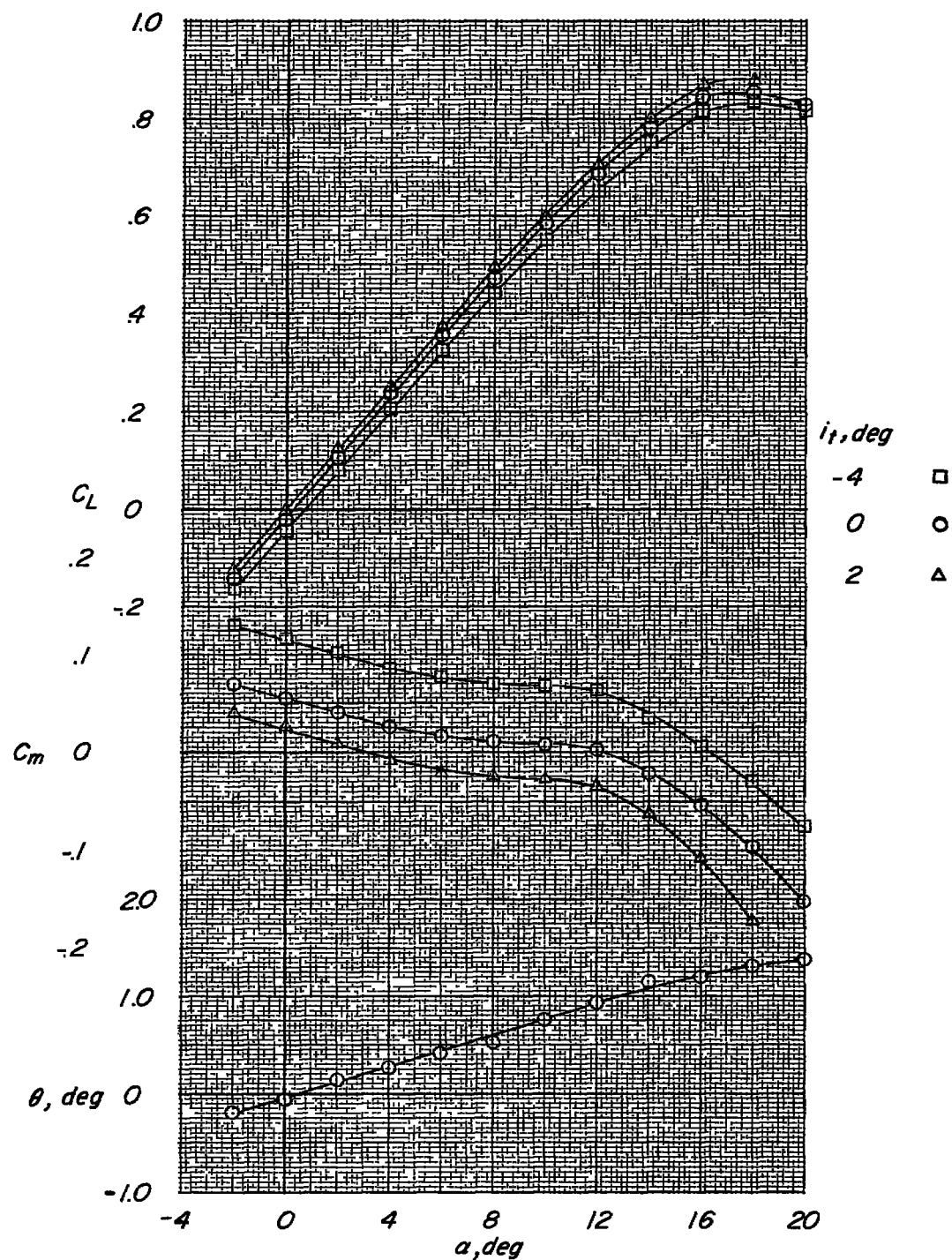Figure 15.- Bomber-model static data.

Figure 16.- Fighter-model static data.   q = 20 lb/ft^2.

BOMBER ALONE
Root locked
236 (890) Flutter at 9.1 cps

COUPLED: TIP TO TIP		
Root locked		
β = 0°; δ/ϕ = 1.09	β = 10°; δ/ϕ = 1.00	β = 20°; δ/ϕ = 0.92
119 (448) Approaching divergence	[a]129 (485) Approaching divergence	64 (240) Neutral oscillations

[a]This condition was also tested with fighter external fuel tanks removed.

COUPLED: FIGHTER ON BOOM		
Root locked		
β = 0°; δ/ϕ = 1.09	β = 10°; δ/ϕ = 1.00	β = 20°; δ/ϕ = 0.92
133 (500) Approaching divergence	125 (470) Approaching divergence	64 (240) Neutral oscillations

BOMBER ALONE
Root free + spring
250 (940) Flutter at 9.5 cps

COUPLED: TIP TO TIP		
Root free + spring		
β = 0°; δ/ϕ = 1.09	β = 10°; δ/ϕ = 1.00	β = 20°; δ/ϕ = 0.92
109 (410) Approaching divergence	144 (540) Approaching divergence	64 (240) to 88 (332) Neutral oscillations

COUPLED: FIGHTER ON BOOM		
Root free + spring		
β = 0°; δ/ϕ = 1.09	β = 10°; δ/ϕ = 1.00	β = 20°; δ/ϕ = 0.92
111 (416) Approaching divergence	No tests	71 (267) to 83 (310) Neutral oscillations

BOMBER ALONE
Root free
250 (940) Flutter at 9.5 cps

COUPLED: TIP TO TIP		
Root free		
β = 0°; δ/ϕ = 1.09	β = 10°; δ/ϕ = 1.00	β = 20°; δ/ϕ = 0.92
118 (445) Approaching divergence	146 (550) Approaching divergence	85 (319) Neutral oscillations

COUPLED: FIGHTER ON BOOM
Root free
No tests

Figure 17.- Summary chart of maximum test speed conditions. Corresponding full-scale simulated speeds in parenthesis. All speeds in miles per hour.